

Hydrogeochemical processes and contaminants enrichment with special emphasis on fluoride in groundwater of Birbhum district, West Bengal, India

Asit Kumar Batabyal¹

Received: 7 December 2015 / Accepted: 22 March 2017 / Published online: 6 April 2017
© Springer-Verlag Berlin Heidelberg 2017

Abstract The hydrogeochemistry of groundwater in rural parts of Birbhum district, West Bengal, India, has been studied to understand the contaminants and prime processes involved in their enrichment with a focus on F^- concentration. The lithological units consist of Quaternary alluviums with underlying Rajmahal basaltic rocks of Middle Jurassic age. Groundwater occurs in the alluviums, weathered residuum and fracture zone of Rajmahal rocks. Studies show elevated concentration of Cl^- , SiO_2 , Fe and F^- ; excess Cl^- is attributed to anthropogenic inputs, SiO_2 is ascribed to high degree of weathering of silica rich host rocks, and high Fe is due to the interaction of water with Fe-rich sediments under reducing condition. The F^- concentration is found high (>1.20 mg/L) mainly in water from Rajmahal rocks revealing a lithological control on F^- enrichment. The weathering of silicates and ion exchange are the leading controlling processes for major ions in groundwater. The F^- enrichment is due to the dissolution of F^- -bearing minerals and perhaps also through anion exchange (OH^- for F^-) on clay minerals at high alkaline conditions; precipitation of $CaCO_3$ favours CaF_2 dissolution leading to elevated F^- concentration. $CaHCO_3$, the dominant water type, contains low F^- while $NaHCO_3$ and $NaCl$ types exhibit high F^- concentrations. Among the three spatial associations, Cluster-1 and Cluster-2 are $CaHCO_3$ type; Cluster-3 shows $NaHCO_3$ and $NaCl$ waters with low Ca^{2+} and Mg^{2+} and high Na^+ contents. Cluster-1 and Cluster-2 waters are, in general, drinkable barring the

elevated Fe content, while Cluster-3 water is unsafe for drinking due to the high F^- concentration.

Keywords Groundwater · Hydrogeochemistry · Fluoride · Cluster analysis · Birbhum district · India

Introduction

Various natural geochemical processes such as weathering, dissolution and ion exchange are responsible for the quality of groundwater including composition of recharge water, host rock mineralogy and climate. Excessive application of chemical fertilizer in agriculture and over-abstraction of groundwater and poor sanitary conditions are the prime anthropogenic inputs for groundwater pollution in rural areas. The hydrogeochemical studies provide a clear understanding of the subsurface geologic environments and the processes involved in the chemical evolution of groundwater.

In Indian context, the groundwater pollution caused two acute health problems arising as a result of higher concentrations of fluoride (F^-) and arsenic (As) (Subba Rao 2011). F^- in drinking water is an essential nutrient for the health of bones and teeth, but it is harmful when the concentration exceeds the permissible limit. According to the World Health Organization (WHO 2011), the maximum permissible limit of F^- in drinking water is 1.5 mg/L. In view of the environmental and socio-economic conditions of the Indian subcontinent and drinking water intake, the safe limit of F^- is considered as 0.6–1.2 mg/L (ISI 1983; Subba Rao 2011). A low content of fluoride ($F^- < 0.6$ mg/L) causes dental carries, whereas fluoride-rich water ($F^- > 1.2$ mg/L) can lead to dental fluorosis, and excessively high concentration of fluoride ($F^- > 3.0$ mg/L) may lead to skeletal fluorosis.

✉ Asit Kumar Batabyal
drakbatabyal@gmail.com

¹ Environmental Engineering Group, CSIR-Central Mechanical Engineering Research Institute, Mahatma Gandhi Avenue, Durgapur 713 209, India

F^- contamination in groundwater is mainly geogenic, and its concentration depends on the amount of F^- in the host rock, the residence time of water, pH, presence or absence of ion complexes and colloids, temperature, solubility of F^- -bearing minerals, anion exchange capacity of the aquifer material (OH^- for F^-), and the presence or absence of Ca^{2+} and HCO_3^- ions in the water (Apambire et al. 1997; Yidana et al. 2012). The F^- is leached into water from the dissolution of various minerals in rocks and soils, such as fluorite (or fluorspar) [CaF_2], fluoroapatite [$Ca_{10}(PO_4)_6F_2$], topaz [$Al_2(F,OH)SiO_4$], amphiboles and micas (Pickering 1985; Handa 1988; Wenzel and Blum 1992; Gaciri and Davies 1993; Bardsen et al. 1996; Subba Rao and Devadas 2003; Chae et al. 2007). The anthropogenic activities like use of phosphatic fertilizer and pesticide, sewage and sludge and depletion of groundwater table have also been indicated to cause an increase in F^- concentration in groundwater (Ramanaiah et al. 2006).

High F^- concentrations are found in many parts of the world, particularly in parts of India, China, Central Africa and South America (WHO 2011). The excess F^- in groundwater was recorded in several states and Union territories of India (Andhra Pradesh, Delhi, Gujarat, Haryana, Karnataka, Madhya Pradesh, Orissa, Punjab, Rajasthan, Tamil Nadu, Uttar Pradesh and West Bengal) (Srinivasa Rao 1997). A total of 60–70 million people in India have been estimated to be at F^- risk (UNICEF 1999).

In West Bengal, the F^- contamination in groundwater was first detected in Birbhum district; the excess F^- is found in several blocks mainly along the western part of the district (Fig. 1). The groundwater occurs in these blocks in different types of hydrogeological formations at various depth-ranges namely, fractured granite (depth 50–80 m), Gondwana sediments (depth within 30 m), basaltic rocks including intertrappean sediments (depth 50–80 m) and older alluvium (depth 50–60 m) (<http://cgwb.gov.in>). During a survey in 2001, it was observed that about 52,563 population spreading over 78 localities were found to be affected by F^- contaminated groundwater (<http://cgwb.gov.in>); fluorosis-related health disorders of the habitants were mainly detected in some villages of Nalhati-I and Rampurhat-I blocks. In these areas, the F^- concentration in groundwater ranges from 0.3 to 20.9 mg/L (Gupta et al. 2006; Patra et al. 2010; Mondal et al. 2014). A small number of published data are available on F^- contamination in groundwater of Birbhum district, particularly in the domain of hydrogeochemistry and sources of elevated F^- ; the present area of investigation is virgin with respect to these studies.

The main objectives of the present investigation are: (1) to characterize the hydrogeochemical properties of groundwater, (2) to identify the contaminants in

groundwater, their spatial distribution patterns and possible sources, (3) to decipher the relationship between F^- and other hydrogeochemical parameters and to presume the relevant geochemical factors controlling the F^- enrichment in groundwater and (4) to understand the water types and spatial associations through hydrogeochemical facies studies and cluster analysis.

Study area

Location, climate, and topography

The Birbhum district lies at the north-eastern end of Chhotanagpur plateau and slopes down to merge with alluvial plains of Ganges. The district is confined in between latitudes $23^{\circ}32'30''N$ and $24^{\circ}35'0''N$ and longitudes $88^{\circ}1'40''E$ and $87^{\circ}5'25''E$ and spreads over an area of 4545 km^2 . The district is surrounded in the north and west by the Jharkhand state, in the east by the districts of Murshidabad and Burdwan and in the south by Burdwan, from which it is separated by the Ajay river (<http://birbhum.gov.in/geog1.htm>).

The present study area, is located in the north-western marginal part of the Birbhum district and includes mainly two adjacent Gram Panchayats (GP)—Haridaspur in Nalhati-I block and Narayanpur in Rampurhat-I block (Fig. 1). Haridaspur GP is situated on the northern bank of the west–east flowing Brahmani river while the Narayanpur GP on the southern bank of the river. The study area covers about 94 km^2 and is encompassed within latitudes $24^{\circ}12'28''N$ – $24^{\circ}17'52''N$ and longitudes $87^{\circ}38'16''E$ – $87^{\circ}47'38''E$. According to national census 2011 (<https://data.gov.in>), the total population of Haridaspur GP is 22,534 and that of Narayanpur GP is 25,264. Groundwater is the main source of drinking water for the rural people, and water is extracted mainly using hand pumps.

The region experiences the semi-arid climatic conditions. The summer season extends from the middle of March to the middle of June, and monsoon season lasts from the middle of June to the middle of October and the winter from the middle of October to the middle of March. The temperature rises up to $45\text{ }^{\circ}C$ in summer and drops to $10\text{ }^{\circ}C$ in winter. Annual average rainfall varies from 600 to 1200 mm.

The study area has an undulating topography with a minimum elevation of 39 m (amsl) and a maximum elevation of 76 m (amsl). In general, the ground surface slopes from west to east direction. The area is traversed by two west–east flowing rivers, Brahmani in the central part and the Tripita River runs in the northern part of the Haridaspur Panchayat (Fig. 1); other water bodies include ponds, a reservoir and a north–south running canal for

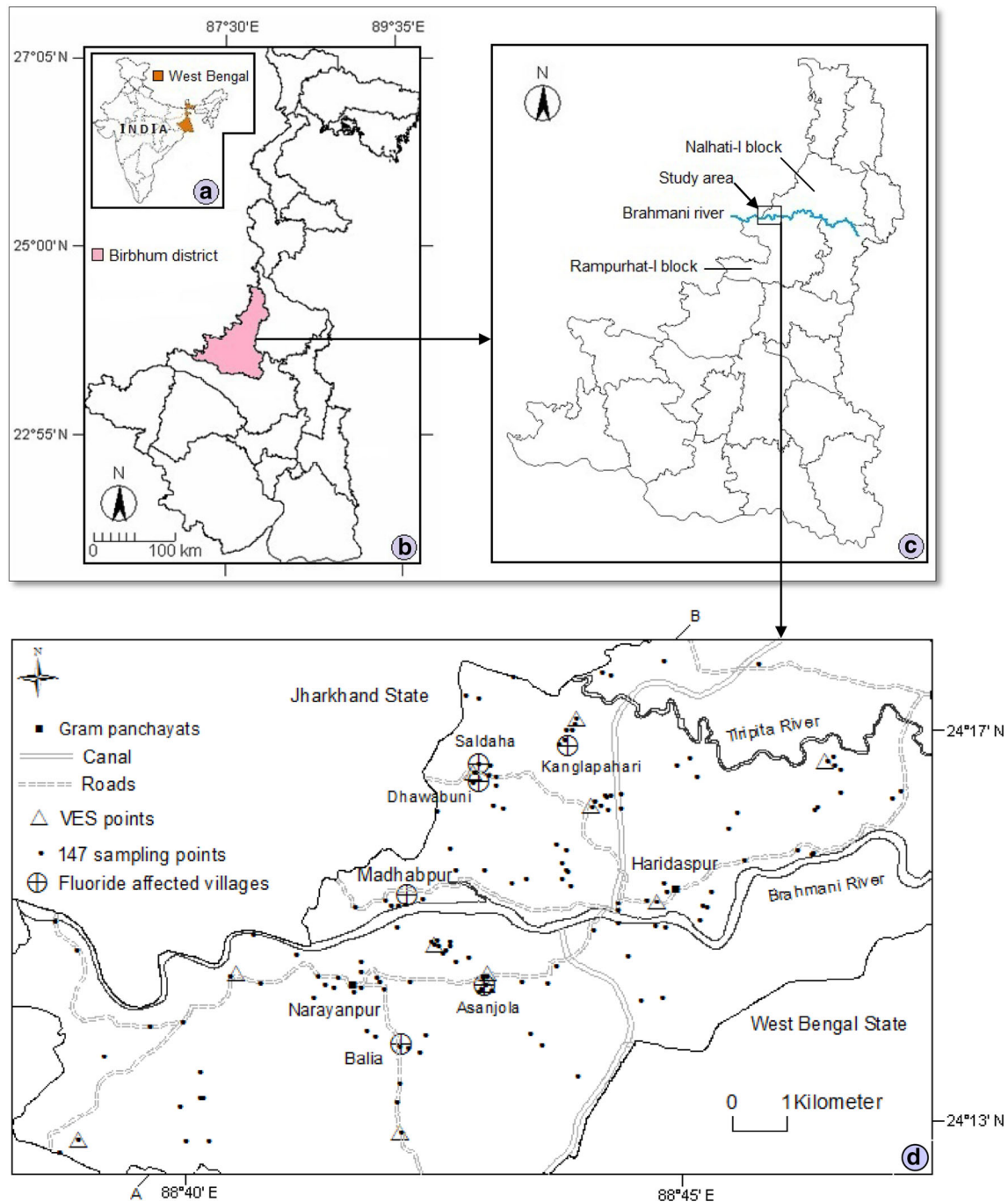


Fig. 1 a India, b West Bengal state, c Birbhumi district showing administrative blocks, d study area showing total 147 groundwater sampling points, 11 VES points and 6 fluoride affected villages

irrigation purposes. Most of the study area is comprised of agricultural land, and farming depends upon rainfall, groundwater and canal water.

Geology and hydrogeology

The stratigraphy of the Birbhumi area as described by Mukherjee et al. (1969) is given in Table 1. The Archaean

rocks comprising of granites and granite–gneiss with enclaves of metamorphics are mainly exposed in the south-western part. The Gondwanas, overlying the Archaean are represented by thick pile of sedimentary rocks belonging to Barakar series (Permian) and Dubarajpur beds (Lower Jurassic). The outcrops of Gondwana rocks are found as patches in the south and south-western part along the Ajoy river (<http://cgwb.gov.in>). The Rajmahal basaltic traps are

Table 1 Stratigraphic sequence in the Birbhum area (Mukherjee et al. 1969)

Formation	Age
Alluvium	Recent
Laterites and lateritic gravel with silicified fossil wood	
Clay beds	Tertiary
Ferruginous and feldspathic sandstones	
Rajmahal traps	Middle Jurassic
Flaggy shales, clays and compact sandstones (Dubrajpur beds)	Lower Jurassic
Sandstones, shales with coal seams (Barakar Series)	Permian (Gondwana)
<i>Unconformity</i>	
Granites, Granite-gneisses, biotite-schists, calc-granulites with quartz and pegmatite veins	Archaean

exposed in the northern and north-western parts of the district. The Tertiary formation is exposed as patches and comprises clay beds, ferruginous and feldspathic sandstones (Mukherjee et al. 1969). The thickness of alluvium increases from west to east, from <20 m to about 80 m below ground level (bgl) in the western part of the district and it increases to huge thickness towards east.

The older alluvium of Upper Tertiary to Lower Quaternary age has extensively covered the eastern and south-eastern parts of the district. Older alluvium with overlying laterite and lateritic soil mainly covers the areas of uplands. Recent alluvium consists of alternating layers of sand, silt, clay of Upper Quaternary age, occurs in the extreme eastern parts of the district as well as along the major river courses (<http://cgwb.gov.in>).

The northern part of the district around Nalhati, west of Rampurhat, Murarai, etc., is underlain by basaltic (Rajmahal volcanic) rocks and the weathered zone of this rock forms the main repository of groundwater in the areas. In the Rampurhat–Nalhati–Murarai tract the ‘depth to water level’ generally varies according to the topography of the area and range from 2.6 to 17.0 mbgl, but usually around 4–12 mbgl (CGWB 1985).

According to yield potentiality and aquifer characteristics in Nalhati area 220 m³/h yield was recorded at 3.4 m drawdown only. Transmissivity is about 2900 m²/d and storativity about 2×10^{-3} , indicating a local confined groundwater condition. Further south of Nalhati near Rampurhat yield of the aquifer is almost same, but drawdown is higher (10 m). Both transmissivity and storativity values reduce to 1750 m²/d and 1.4×10^{-3} , respectively (CGWB 1985).

Based on the data obtained from the vertical electrical sounding (VES) at 11 locations, logs of boreholes drilled

by the Public Health Engineering Department (PHED), Govt. of West Bengal in and around the study area and field studies, it is observed that the study area is mainly covered by the older and recent alluviums along with laterites and lateritic soil at places. At maximum locations, at the top of stratigraphic column a clay or sandy clayey bed is recorded after the soil cover. The Rajmahal Trap basalts act as the basement of the overlying alluviums at majority of the study area. From the field survey, it is also observed that the Rajmahal Trap basalts are exposed at places in the western marginal part; the depth of occurrence of the trap generally increases from the west to the east. The hydrogeological profile constructed based on VES data along SW–NE direction provides an idea of the subsurface environment of the study area (Fig. 2).

The piezometric data were collected from 109 tube wells where strainers were placed at depths ranging between 14.02 and 97.54 m. The groundwater is found in the alluvium zone, weathered residuum and in the fracture zone of Rajmahal rocks. In the western marginal fringe of the study area, the tube wells mainly reach the weathered residuum or water-bearing fractures in Rajmahal rocks at shallow depths; in the eastern part, several tube wells are installed at greater depths (50–90 m, bgl) probably to tap sufficient water from the granular zone or fissured formation (Rajmahal rocks). The depth of groundwater level (piezometric surface below ground level) ranges from 0.54 to 22.69 m; at greater part (83.63%), the groundwater level is within 10 m. The piezometric surface with respect to mean sea level (msl) varies from 27.82 to 71.71 m; the contour map of piezometric surface (Fig. 3) shows the groundwater flow pattern in the study area. Two tube wells (location 13 and 30) are found to be under artesian well conditions.

Materials and methods

Surface geophysical investigation

The vertical electrical sounding (VES) was carried out using the instrument DDR3 Resistivity Meter, a specialized version of resistivity meters of IGIS, Hyderabad, India, at 11 points, 6 in Narayanpur GP and 5 in Haridaspur GP. The basic objective of the study was to unfold the subsurface geology and basement configuration of the study area. Schlumberger sounding array with a maximum electrode separation of 300 m was used in the investigation to obtain the vertical variation of resistivity along depth.

Water sample collection

Groundwater quality studies have been carried out based on 147 tube wells spreading over 49 villages of the study

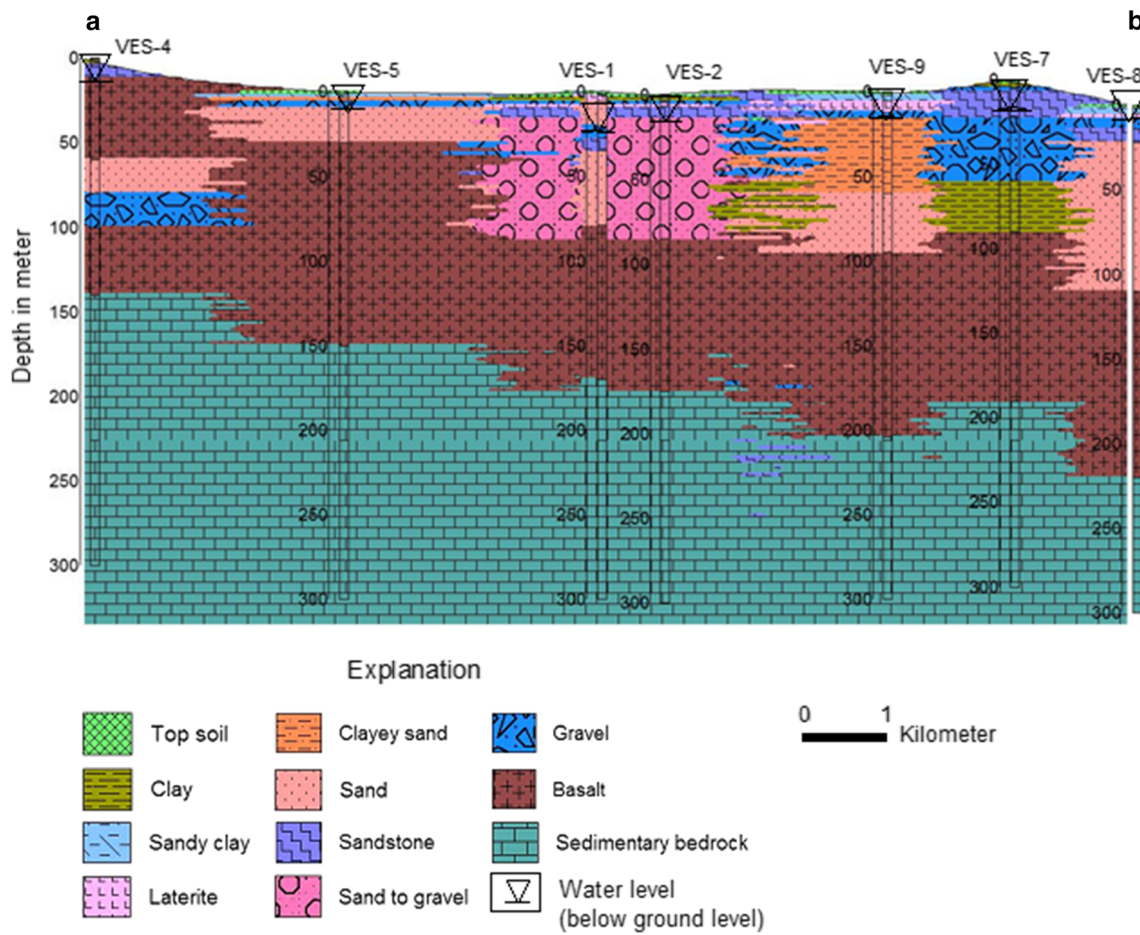


Fig. 2 Hydrogeological cross section along the A–B line (Fig. 1d)

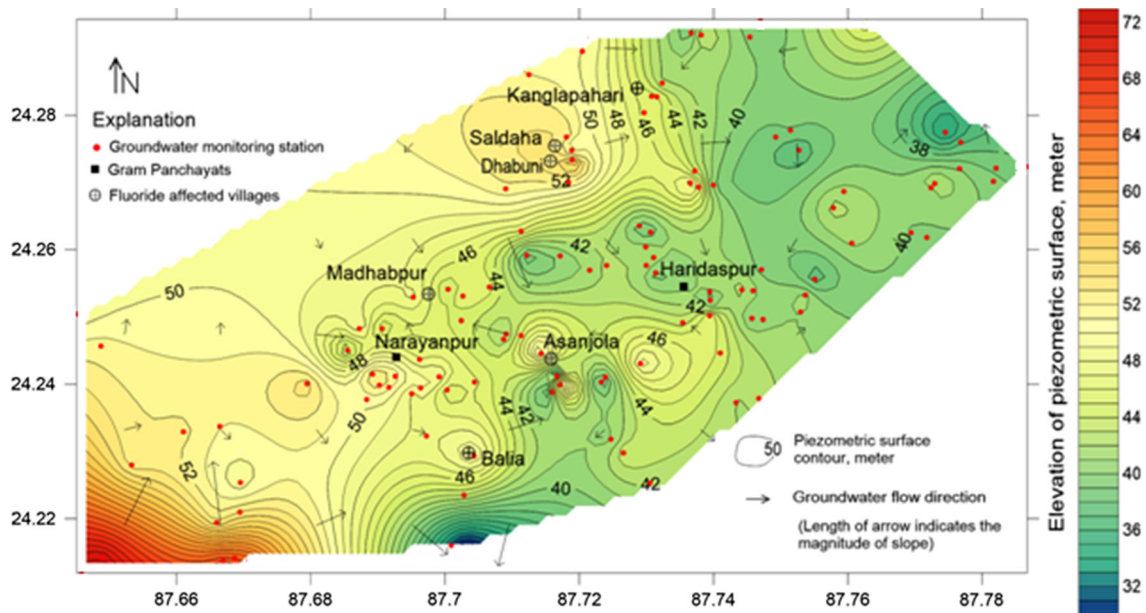


Fig. 3 Contour map showing elevation of piezometric surface with respect to mean sea level

area (Table 6) during November to December 2014. The water of the tube wells is used for drinking and other domestic purposes without treatment. The geographical coordinates of the tube wells were recorded using a hand-held GPS (GARMIN GPA MAP 78s) and groundwater samples were collected for three purposes—(1) water samples (100 ml) from 147 tube wells basically to measure the F^- concentration, (2) representative 31 samples (2.5 L) selected from 147 tube wells for detailed chemical analysis including trace metals and (3) water samples (100 ml) from nine ponds for the measurement of chloride (Cl^-) concentration. The groundwater samples were collected after 10–15 min of pumping of the tube wells and stored in pre-cleaned new polyethylene bottles after filtration to remove particulates. All the bottles were re-washed and rinsed before sampling with the water of the concerned tube well to be sampled. All sample bottles were sealed and returned to the laboratory within 24 h and placed in a 4 °C environment for preservation until analyses were completed. The tube well depths were obtained from the available Panchayat office records, through interviews with the village people and in some cases from the local mechanics who installed the tube wells.

Analytical methods

The pH, electrical conductivity (EC) and total dissolved solids (TDS) were analysed in the field using a portable multi-parameter tester 35 series (Model—Eutech PCSTEST35). F^- concentration was measured by the fluoride ion selective electrode (Potentiometric method, Bench top ion meter, Model—Thermo Scientific Orion Star A214). All other water parameters, such as total alkalinity as $CaCO_3$ (TA), total hardness as $CaCO_3$ (TH), silica (SiO_2), phosphate (PO_4^{3-}), bromide (Br^-), boron (B), major cations—sodium (Na^+), potassium (K^+), calcium (Ca^{2+}) and magnesium (Mg^{2+}), major anions—bicarbonate (HCO_3^-), chloride (Cl^-), nitrate (NO_3^-) and sulphate (SO_4^{2-}) and trace metals such as arsenic (As), aluminium (Al), cadmium (Cd), chromium (Cr), copper (Cu), iron (Fe), lead (Pb), manganese (Mn), mercury (Hg), nickel (Ni), zinc (Zn), lithium (Li) and strontium (Sr) were determined following the standard procedures as recommended by American Public Health Association (APHA 2005). The analytical precision for the measurements of cations and anions was determined by calculating ionic charge balance error which varied within $\pm 10\%$ (Srinivasamoorthy et al. 2008); 71% of samples show ion balance error within $\pm 5\%$.

Geochemical and statistical analysis

In view of the suitability of groundwater for human consumption, the percent compliance of the groundwater

physicochemical data with respect to Indian Standard (BIS 1991; WHO 2011) was evaluated. The software Surfer 12 was applied to generate spatial distribution pattern of the groundwater contaminants. The Piper diagram (Piper 1944) was generated through AquaChem version 2014.1 software in order to decipher the hydrochemical facies and water types. The potential relationship between various physicochemical parameters was established from the Pearson correlation coefficient generated using the software “Statistical Package for Social Science (SPSS).” The saturation index (SI) of calcite ($CaCO_3$) and fluorite (CaF_2) in the groundwater samples was calculated using PHREEQC interactive (Parkhurst and Appelo 1999), a geochemical software of the US Geological Survey, version 3.3.3.

Q-mode hierarchical cluster analysis (HCA) was performed with the help of software Systat 13. In the present investigation, 31 groundwater samples have been considered for the Q-mode HCA. The variables chosen were the 18 major water parameters, such as pH, EC, TDS, TA, TH, SiO_2 , Na^+ , K^+ , Ca^{2+} , Mg^{2+} , Cl^- , F^- , NO_3^- , SO_4^{2-} , HCO_3^- , Fe, Mn and PO_4^{3-} . The output of the analysis is presented as dendrogram (Fig. 9). The phenon line is drawn across the dendrogram (shown as dotted line) at a linkage distance of 150 to distinguish the number of broad clusters.

Results and discussion

Overall groundwater chemistry and quality

The location and detailed physicochemical data of 31 groundwater samples are given in Table 2. The statistical analyses (minimum, maximum, mean, median and standard deviation) along with a comparison of the data in respect of drinking water standards and correlation coefficient matrix of the physicochemical parameters are presented in Tables 3 and 4, respectively.

Physical properties The pH of the study area varies from 6.67 to 9.98 (mean 8.63) revealing the alkaline nature of groundwater. The EC (201–577 $\mu S/cm$) and TDS (140–415 mg/L) values indicate the low to moderate mineralization in the study area; TDS concentration also reveals that the groundwater is hydro-chemically fresh water type (Table 5) and water is suitable for drinking (Table 3). Total alkalinity (TA) ranges from 71.4 to 295.8 mg/L (mean 153 mg/L); 74.2% of samples show TA within the desirable limit (200 mg/L) (BIS 1991). In respect of total hardness (TH) values (8.24–234.84 mg/L), the water is safe for drinking (Table 3) and indicative of moderately hard (41.94%) to hard (38.71%) types of water at majority of the locations (Table 5).

Major cations and anions Based on the average concentrations, the distribution pattern of the major cations

Table 2 Sample location and results of physicochemical analysis

Sample no.	Longitude	Latitude	pH	EC	TDS	TA	TH	SiO ₂	Na ⁺	K ⁺	Ca ²⁺	Mg ²⁺	Cl ⁻	F ⁻	NO ₃ ⁻	SO ₄ ²⁻	HCO ₃ ⁻
1	87.74734	24.24958	7.02	274	195	102	119.48	40.48	25	1.2	25.66	7.88	13.86	0.2	BDL	4	124.44
6	87.74334	24.23724	6.84	308	219	132.6	131.84	47.98	15.63	BDL	33	11.87	23.75	0.28	3.5	5.06	161.77
8	87.72914	24.24311	7.62	488	351	295.8	222.48	54	27.28	BDL	52.74	21.75	10.89	0.33	1.6	5.47	360.88
10	87.73274	24.22461	6.9	445	315	183.6	169	43	23.12	BDL	42.84	14.83	23.75	0.34	0.86	10.62	224
13	87.71716	24.23991	9.98	562	352	81.6	12.36	45.34	108.31	1.1	3.3	1	98.97	15.6	BDL	8.85	99.55
14	87.71669	24.24117	6.92	317	231	173.4	131.84	45	19.4	BDL	34.61	10.88	13.86	0.28	0.5	5.51	211.55
21	87.70869	24.24667	9.84	536	371	71.4	8.24	40.3	93.21	BDL	2.47	0.5	99	14.8	BDL	7.94	87.11
28	87.71134	24.24722	8.55	525	377	153	160.68	51.46	31.05	BDL	46.14	10.88	69.28	0.22	BDL	10.62	186.66
34	87.70433	24.22930	6.67	535	375	132.6	189.52	49.48	29.5	1.1	56.03	11.87	84.12	0.14	6	20.5	161.77
36	87.70297	24.21526	8.71	577	415	173.4	16.48	36.62	130.85	2	4.94	1	79.18	2.3	BDL	4.07	211.55
43	87.70240	24.24945	8.75	266	190	132.6	103	49.44	21.43	BDL	26.37	8.9	13.86	0.23	BDL	4	161.77
48	87.69504	24.23863	8.78	460	326	234.6	156.56	57.96	48.86	1.5	39.55	13.84	19.8	0.94	BDL	2.3	286.21
58	87.64513	24.25042	8.54	328	232	173.4	127.72	47.22	27.44	BDL	34.61	9.9	9.9	0.22	BDL	5.5	211.55
61	87.66692	24.21374	9.22	421	308	244.8	234.84	58.5	18.54	BDL	57.68	21.75	23.75	0.18	BDL	4.24	298.66
66	87.64584	24.21191	8.72	201	140	71.4	78.28	96.7	10.52	BDL	21.42	5.93	29.69	0.16	7.1	4.28	87.11
69	87.66648	24.23371	9.28	450	320	255	140.1	68.72	55.18	1.5	36.26	11.87	19.79	0.73	BDL	2.26	311.1
72	87.72327	24.24033	9.24	350	245	204	185.4	50.36	15.56	BDL	48	15.82	9.9	0.26	BDL	7	248.88
74	87.72896	24.26352	9.5	460	325	224.4	214.24	56.64	36.83	1.2	51.1	20.76	39.58	0.23	BDL	5.4	273.77
83	87.71714	24.25909	8.5	295	198	204	152.4	44.88	34.4	1.7	38	13.84	19.8	0.29	BDL	5.9	248.88
91	87.69530	24.25295	8.2	272	190	153	123.6	44.68	19.5	11.1	29.66	11.87	17.81	0.26	BDL	8.6	186.66
103	87.75363	24.25324	8.2	208	150	81.6	34.61	43.58	17.4	2.5	21.42	7.91	23.75	0.26	BDL	12.63	99.55
107	87.73652	24.26990	9.25	450	316	224.4	164.8	39.06	56.7	12.7	36.26	17.8	59.38	1	BDL	11.2	273.77
117	87.73158	24.28278	9.4	456	320	91.8	24.72	27.12	71.6	1.6	5.6	1.5	34.64	5.1	BDL	6.34	112
120	87.73230	24.28477	9.3	530	370	142.8	12.36	22.92	130.4	3.4	3.3	1	79.18	5.9	BDL	6.8	174.2
123	87.71899	24.27336	9.6	345	250	102	127.72	36.4	18.8	1.6	33	10.88	29.69	0.13	4.8	10.6	124.44
129	87.71809	24.27678	9.12	510	370	102	173.04	59.5	25.9	1.6	41.2	16.8	49.48	0.22	27.1	26.34	124.44
136	87.75272	24.27483	9.2	278	190	153	111.24	47.34	31.8	1.3	31.31	7.91	9.9	0.22	BDL	6.34	186.66
138	87.75783	24.26625	9.13	260	185	112.2	123.6	52.52	14.4	1.1	31.31	10.88	23.75	0.17	BDL	12.51	136.88
144	87.78672	24.27234	8.8	340	242	91.8	119.48	33.12	17.1	1.1	28.02	11.87	52.43	0.25	BDL	25.27	111.99
149	87.77661	24.27206	8.92	280	210	102	119.48	39.66	13.7	1.1	31.31	9.9	39.58	0.16	BDL	8.44	124.44
152	87.77180	24.26178	8.9	409	290	142.8	160.68	34.04	21.2	4.8	46.14	10.88	54.43	0.18	BDL	7.24	174.22

Sample no.	As	Al	Cd	Cr	Cu	Fe	Pb	Mn	Hg	Ni	Zn	Br ⁻	B	Li	PO ₄ ³⁻	Sr	Na ⁺ /Ca ²⁺	TZ ⁺ /Cl ⁻	CBE (%)
1	BDL	BDL	BDL	BDL	BDL	2.65	BDL	0.76	BDL	BDL	BDL	BDL	BDL	BDL	0.14	BDL	0.85	7.79	9.49
6	BDL	BDL	BDL	BDL	BDL	0.07	BDL	BDL	BDL	BDL	BDL	BDL	BDL	BDL	0.1	BDL	0.41	4.96	-2.31
8	BDL	BDL	BDL	BDL	BDL	0.08	BDL	BDL	BDL	BDL	BDL	BDL	BDL	BDL	0.23	BDL	0.45	18.33	-6.10

Table 2 continued

Sample no.	As	Al	Cd	Cr	Cu	Fe	Pb	Mn	Hg	Ni	Zn	Br ⁻	B	Li	PO ₄ ³⁻	Sr	Na ⁺ /Ca ²⁺	TZ ⁺ /Cl ⁻	CBE (%)
10	BDL	BDL	BDL	BDL	BDL	0.15	BDL	BDL	BDL	BDL	BDL	BDL	BDL	BDL	0.25	BDL	0.47	6.55	-2.12
13	BDL	BDL	BDL	BDL	BDL	0.09	BDL	BDL	BDL	BDL	BDL	BDL	BDL	BDL	0.22	BDL	28.61	1.79	3.89
14	BDL	BDL	BDL	BDL	BDL	0.14	BDL	BDL	BDL	BDL	BDL	BDL	BDL	BDL	0.22	BDL	0.49	8.92	-6.59
21	BDL	BDL	BDL	BDL	0.028	0.18	BDL	BDL	BDL	BDL	BDL	BDL	BDL	BDL	0.08	BDL	32.9	1.52	-1.72
28	BDL	BDL	BDL	BDL	BDL	0.07	BDL	0.19	BDL	BDL	BDL	BDL	BDL	BDL	0.36	BDL	0.59	2.34	-6.82
34	BDL	BDL	BDL	BDL	BDL	0.32	BDL	BDL	BDL	BDL	BDL	BDL	BDL	BDL	0.36	BDL	0.46	2.14	-4.36
36	BDL	BDL	BDL	BDL	BDL	0.69	BDL	BDL	BDL	BDL	0.05	BDL	BDL	BDL	0.33	BDL	23.09	2.72	2.37
43	BDL	BDL	BDL	BDL	BDL	0.17	BDL	0.14	BDL	BDL	BDL	BDL	BDL	BDL	0.4	BDL	0.71	7.68	-2.08
48	BDL	BDL	BDL	BDL	BDL	1.2	BDL	0.027	BDL	BDL	BDL	BDL	BDL	BDL	0.47	BDL	1.08	9.45	-0.25
58	BDL	BDL	BDL	BDL	BDL	0.02	BDL	BDL	BDL	BDL	BDL	BDL	BDL	BDL	0.4	BDL	0.69	13.46	-1.41
61	BDL	BDL	BDL	BDL	BDL	0.22	BDL	0.15	BDL	BDL	BDL	BDL	BDL	BDL	0.33	BDL	0.28	8.2	-1.45
66	BDL	BDL	BDL	BDL	BDL	0.44	BDL	0.04	BDL	BDL	BDL	BDL	BDL	BDL	0.99	BDL	0.43	2.43	-9.58
69	BDL	BDL	BDL	BDL	BDL	0.57	BDL	0.05	BDL	BDL	BDL	BDL	BDL	BDL	0.32	BDL	1.33	9.36	-4.43
72	BDL	BDL	BDL	BDL	BDL	0.1	BDL	0.07	BDL	BDL	BDL	BDL	BDL	BDL	BDL	BDL	0.28	15.74	-1.26
74	BDL	BDL	BDL	BDL	BDL	0.12	BDL	0.28	BDL	BDL	BDL	BDL	BDL	BDL	0.33	BDL	0.63	5.28	1.46
83	BDL	BDL	BDL	BDL	BDL	0.06	BDL	0.32	BDL	BDL	BDL	BDL	BDL	BDL	BDL	BDL	0.79	8.19	-2.04
91	BDL	BDL	BDL	BDL	BDL	0.36	BDL	0.55	BDL	BDL	BDL	BDL	BDL	BDL	BDL	BDL	0.57	7.14	-2.14
103	BDL	BDL	BDL	BDL	BDL	0.1	BDL	0.022	BDL	BDL	BDL	BDL	BDL	BDL	BDL	BDL	0.71	3.79	-0.57
107	BDL	BDL	BDL	BDL	BDL	1.9	BDL	1.02	BDL	BDL	BDL	BDL	BDL	BDL	BDL	BDL	1.36	3.62	-2.69
117	BDL	BDL	BDL	BDL	BDL	0.11	BDL	BDL	BDL	BDL	BDL	BDL	BDL	BDL	BDL	BDL	11.15	3.64	9.35
120	BDL	BDL	BDL	BDL	BDL	0.35	BDL	BDL	BDL	BDL	BDL	BDL	BDL	BDL	BDL	BDL	34.45	2.69	6.86
123	BDL	BDL	BDL	BDL	BDL	2.38	BDL	0.06	BDL	BDL	0.06	BDL	BDL	BDL	0.19	BDL	0.5	4.06	3.43
129	BDL	BDL	BDL	BDL	BDL	0.87	BDL	BDL	BDL	BDL	BDL	BDL	BDL	BDL	0.24	BDL	0.55	3.3	2.04
136	BDL	BDL	BDL	BDL	BDL	BDL	BDL	0.13	BDL	BDL	BDL	BDL	BDL	BDL	0.48	BDL	0.89	13	2.17
138	BDL	BDL	BDL	BDL	BDL	0.19	BDL	BDL	BDL	BDL	BDL	BDL	BDL	BDL	0.28	BDL	0.4	4.64	-1.06
144	BDL	BDL	BDL	BDL	0.064	29.84	BDL	1.53	BDL	BDL	0.54	BDL	BDL	BDL	0.27	BDL	0.53	2.13	-9.57
149	BDL	BDL	BDL	BDL	BDL	8.19	BDL	1.18	BDL	BDL	BDL	BDL	BDL	BDL	0.28	BDL	0.38	2.69	-5.30
152	BDL	BDL	BDL	BDL	BDL	12	BDL	0.5	BDL	BDL	0.45	BDL	BDL	BDL	0.25	BDL	0.4	2.76	-3.46

pH in numeric units; EC in $\mu\text{S}/\text{cm}$; all other parameters in mg/L ; $\text{Na}^+/\text{Ca}^{2+}$ and TZ^+/Cl^- in meq/L ; BDL stands for below detection limit (K^+ , Li and Sr < 1; NO_3^- < 0.4; Br < 2; B < 0.5; PO_4 and Fe < 0.05; As, Al, Cr and Ni < 0.01; Cd < 0.002; Mn, Zn and Cu < 0.02; Pb < 0.005; Hg < 0.001); TZ^+ stands for total cation; CBE stands for charge balance error

and anions may be ordered as $\text{Na}^+ > \text{Ca}^{2+} > \text{Mg}^{2+} > \text{K}^+$ and $\text{HCO}_3^- > \text{Cl}^- > \text{SO}_4^{2-} > \text{NO}_3^-$, respectively. Ca^{2+} ranges from 2.47 to 57.68 mg/L, whereas Mg^{2+} varies from 0.5 to 21.75 mg/L and both the ions are within the desirable limit (Table 3). Na^+ is the leading cation in the study area, ranging from 10.52 to 130.85 mg/L (mean 39.05 mg/L). In potable water, the concentration of K^+ ranges from 1 mg/L or less to about 20 mg/L; it maintains the fluid balance in the body. In the present investigation the K^+ content is recorded as below detection limit (<1 mg/L) to 12.7 mg/L. HCO_3^- is the dominant anion, ranging from 87.11 to 360.88 mg/L (mean 186.6 mg/L). The content of HCO_3^- in drinking water has no known adverse health effects. The Cl^- concentration varies from 9.9 to 99 mg/L (mean 37.96 mg/L) which is below the desirable limit of 250 mg/L for drinking purposes, but with respect to fresh water, the Cl^- content at maximum locations in the study area is high (>10 mg/L, about 93% of samples); the origin of excess Cl^- in groundwater is discussed in a later section. The spatial distribution of Cl^- in groundwater of the study area is shown in Fig. 4a. The SO_4^{2-} concentrations were recorded as 2.26–26.34 mg/L, well below the desirable limit (200 mg/L). In the present study area, the NO_3^- content is below the detection limit (<0.4 mg/L) at majority locations (74.19% sites). At the

rest of the sites, the NO_3^- concentration varies from 0.5 to 27.1 mg/L. The F^- concentration (based on analysis of 147 groundwater samples) ranges from 0.023 to 19 mg/L (mean 1.06 mg/L, median 0.2 mg/L). The detailed discussion on F^- content in groundwater is incorporated in later sections. The Br^- concentration in the study area is found to be below the detection limit (<2 mg/L). B is also recorded as below the detection limit (<0.5 mg/L).

Phosphate and silica Phosphate (PO_4^{3-}) gets adsorbed or fixed as aluminium or iron phosphate in acidic soils or as calcium phosphate in alkaline or neutral soils; as a result, the concentration of PO_4^{3-} in groundwater is usually low, but various chemical processes in soil strata may induce the mobility of PO_4^{3-} in subsoil and groundwater (Jain et al. 2010). The PO_4^{3-} in groundwater of the study area is found below the detection limit (<0.05 mg/L) at certain places (22.58%); in the rest cases, it ranges from 0.08 to 0.99 mg/L. The low concentration indicates that most probably the source of PO_4^{3-} in groundwater is not from the application of fertilizer for agriculture.

Silica (SiO_2) in groundwater is almost exclusively and unequivocally a result of water–rock interaction (Hem 1985). Therefore, the SiO_2 content of groundwater increases due to increased contact with silicate rocks and is directly proportional to the residence time of groundwater.

Table 3 Statistical summary of the physicochemical parameters of groundwater samples and comparison with the drinking water standards (BIS 1991; WHO 2011)

Parameters	Min	Max	Mean	Median	SD	Indian standard (BIS 1991)	WHO limit (WHO 2011)
pH	6.67	9.98	8.63	8.8	0.92	6.5–8.5 (29.03%)	7–8 (6.45%)
EC	201	577	391.48	409	112.33	–	–
TDS	140	415	276.39	290	77.97	500 (100%)	1000 (100%)
TA	71.4	295.8	153	142.8	60	200 (74.2%)	–
TH	8.24	234.84	124.19	127.72	63.18	300 (100%)	–
SiO_2	22.92	96.7	47.23	45.34	13.38	–	–
Na^+	10.52	130.85	39.05	25.9	33.52	–	–
K^+	<1	12.7	2.13	1.1	2.74	–	–
Ca^{2+}	2.47	57.68	32.04	33	15.6	75 (100%)	75 (100%)
Mg^{2+}	0.5	21.75	10.78	10.88	5.84	30 (100%)	30 (100%)
Cl	9.9	99	37.96	23.75	27.34	250 (100%)	250 (100%)
F^-	0.023	19	1.06	0.2	3.30	1.20 (91.83%)	1.5 (92.3%)
NO_3^-	<0.4	27.1	1.96	0.4	4.98	45 (100%)	50 (100%)
SO_4^{2-}	2.26	26.34	8.57	6.8	5.89	200 (100%)	250 (100%)
HCO_3^-	87.11	360.88	186.66	174.22	73.2	–	–
Cu	<0.02	0.06	0.02	0.02	0.01	0.05 (96.8%)	0.05 (96.8%)
Fe	<0.05	29.84	2.06	0.19	5.75	0.3 (54.8%)	0.3 (54.8%)
Mn	<0.02	1.53	0.23	0.04	0.39	0.1 (61.3%)	0.1 (61.3%)
Zn	<0.02	0.54	0.05	0.02	0.12	5 (100%)	3 (100%)
PO_4^{3-}	<0.05	0.99	0.25	0.25	0.19	–	–

pH in numeric units, EC in $\mu\text{S}/\text{cm}$, all other parameters in mg/L; statistics of F^- based on analysis of 147 groundwater samples and permissible limit of F^- is set at 1.20 mg/L (ISI 1983; Subba Rao 2011); the figure within parenthesis indicates per cent compliance

Min minimum, Max maximum, SD standard deviation

Table 4 Correlation coefficient matrix of physicochemical parameters of groundwater samples

	pH	EC	TDS	TA	TH	Na ⁺	K ⁺	Ca ²⁺	Mg ²⁺	Cl ⁻	F ⁻	NO ₃ ⁻	SO ₄ ²⁻	HCO ₃ ⁻	Fe	Mn	PO ₄ ³⁻
pH	1	0.206	0.176	-0.097	-0.287	0.388*	0.088	-0.327	-0.203	0.293	0.441*	-0.011	-0.040	-0.097	0.065	0.033	0.011
EC		1	0.955**	0.278	0.050	0.632**	-0.024	-0.016	-0.035	0.642**	0.457**	0.139	0.079	0.278	-0.083	-0.182	-0.071
TDS			1	0.278	0.022	0.640**	-0.025	-0.007	-0.019	0.665**	0.418*	0.167	0.142	0.279	-0.103	-0.228	-0.137
TA				1	0.644**	-0.031	0.141	0.591**	0.673**	-0.353	-0.355	-0.236	-0.394*	1.000**	-0.232	-0.108	-0.024
TH					1	-0.639**	0.023	0.974**	0.945**	-0.426*	-0.635**	0.165	0.100	0.644**	0.029	0.130	0.116
Na ⁺						1	0.081	-0.680**	-0.608**	0.673**	0.707**	-0.158	-0.185	-0.030	-0.182	-0.223	-0.213
K ⁺							1	-0.025	0.120	0.087	-0.067	-0.088	0.056	0.141	0.018	0.381*	-0.344
Ca ²⁺								1	0.901**	-0.408*	-0.666**	0.150	0.129	0.591**	0.012	0.062	0.150
Mg ²⁺									1	-0.463**	-0.600**	0.177	0.128	0.672**	0.031	0.161	0.006
Cl ⁻										1	0.674**	0.094	0.342	-0.354	0.131	0.041	-0.102
F ⁻											1	-0.077	-0.033	-0.354	-0.125	-0.207	-0.230
NO ₃ ⁻												1	0.575**	-0.235	-0.071	-0.178	0.156
SO ₄ ²⁻													1	-0.396*	0.472**	0.299	-0.127
HCO ₃ ⁻														1	-0.236	-0.111	-0.024
Fe															1	0.762**	0.013
Mn																1	-0.136
PO ₄ ³⁻																	1

Bold values: significant correlation, * correlation is significant at the 0.05 level (2-tailed); ** correlation is significant at the 0.01 level (2-tailed)

Table 5 Groundwater classifications based on TDS and total hardness

Classification		Number of samples	Percentage of samples
Based on TDS (mg/L) (Davis and DeWiest 1966)			
<500	Desirable for drinking	31	100
500–1000	Permissible for drinking	Nil	Nil
1000–3000	Useful for irrigation	Nil	Nil
>3000	Unfit for drinking and irrigation	Nil	Nil
Based on TDS (mg/L) (Freeze and Cherry 1979)			
<1000	Fresh water type	31	100
1000–10,000	Brackish water type	Nil	Nil
10,000–100,000	Saline water type	Nil	Nil
>100,000	Brine water type	Nil	Nil
Based on total hardness as CaCO ₃ (mg/L) (Sawyer and McCarty 1967)			
<75	Soft	6	19.35
75–150	Moderately hard	13	41.94
150–300	Hard	12	38.71
>300	Very hard	Nil	–

SiO₂ is found in the crystalline and amorphous states; the three most common crystalline forms are quartz, cristoballite and tridymite. The amount of SiO₂ released into the water is controlled by different factors, such as water saturation deficit of the aeration zone, seasonal fluctuations of precipitation and temperature (evapotranspiration), bed-rock reactivity and mineral stability (Dobrzynski 2005). Average concentration of SiO₂ in natural water ranges between 1.0 and 30.0 mg/L (Davis 1964). The solubility of quartz and amorphous silica is described by Eq. 1 (Appelo and Postma 2005):



H₄SiO₄ remains undissociated at pH values below 9, and the stability of SiO_{2(s)} phases is determined by the solubility product of Eq. 1.

$$K = [\text{H}_4\text{SiO}_4] \quad (2)$$

For quartz, $K = 10^{-3.98}$ at 25 °C; the most soluble phase is amorphous SiO_{2(s)} which has a solubility product of about $10^{-2.7}$ (25 °C) (Appelo and Postma 2005).

The present investigation is carried out in a tropical region; the SiO₂ content in groundwater samples ranges from 22.92 to 96.7 mg/L with the mean and median values of 47.23 and 45.34 mg/L, respectively. The relatively high values imply that SiO₂ is one of the major chemical components of the groundwater. The high values of SiO₂ must have been favoured by both the high SiO₂ content of the host parent rocks and high degree of weathering that characterizes the tropical regions.

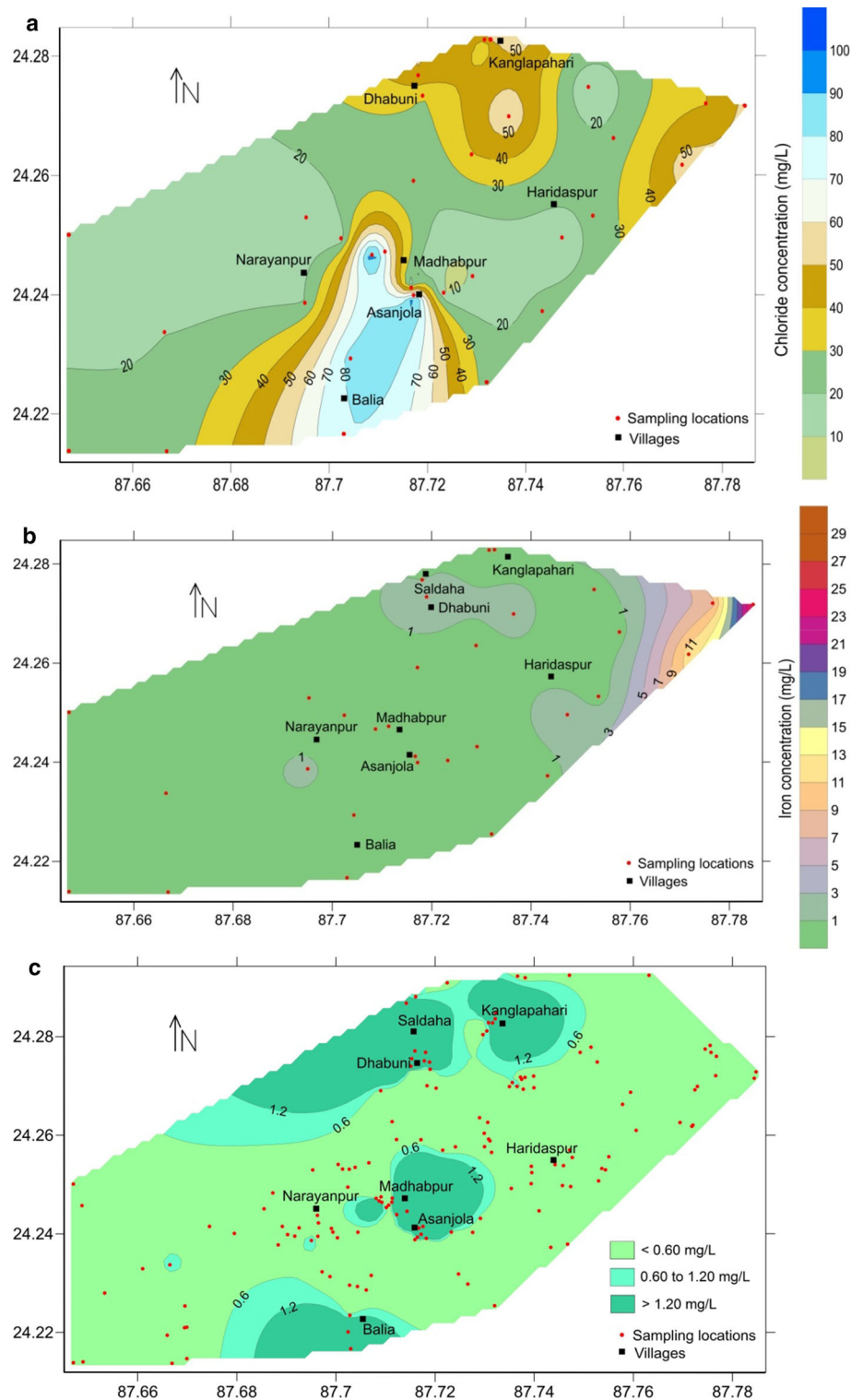
There are some activities related to crushing of stones in and around the study area; the basement rock (basalt) is mined and crushed to different sizes for uses in construction of roads and buildings. The infiltration of surface water

contaminated with air borne SiO₂ generated from nearby quarries and crushing sites probably also have a role in the high concentration of SiO₂ at some places. The effects of consumption of excessive amount of dissolved SiO₂ to health are not yet properly known.

Trace metals In the present investigation, the concentration of trace metals viz. As, Al, Cd, Cr, Pb, Hg, Ni, Li and Sr was found below the detection limits (As, Al, Cr and Ni < 0.01 mg/L; Cd < 0.002 mg/L; Pb < 0.005 mg/L; Hg < 0.001 mg/L; Li and Sr < 1.0 mg/L). However, Fe, Mn, Zn and Cu were detected in 93.55, 58.07, 12.91 and 16.13% of the groundwater samples, respectively. The abundance of the detected trace metals in the groundwater samples can be ordered as, Fe > Mn > Zn > Cu (Table 3).

In groundwater system, iron (Fe) occurs in one of two oxidation states—reduced soluble divalent ferrous iron (Fe²⁺) or oxidized insoluble trivalent ferric iron (Fe³⁺). When groundwater comes in contact with oxygen of the atmosphere, the Fe is oxidized to the ferric state and is precipitated as an iron-mineral, such as ferric hydroxide, Fe(OH)₃. The origin of Fe in groundwater is due to the leaching of Fe from the soil and rock formations during permeation of rain water to subsurface. The subsurface redox conditions have also significant influence on the Fe content of groundwater; the removal of dissolved oxygen by organic matter within the sediments creates a reduced state in the subsurface. Under the reducing environment, the solubility of Fe-bearing minerals increases, leading to enrichment of the dissolved iron in the groundwater. In present investigation, the concentration of Fe ranges from below detection limit (<0.05 mg/L) to 29.84 (mean 2.06), and shows poor compliance (54.8%) with respect to drinking water standards (BIS 1991; WHO 2011) (Table 3). The elevated concentration of Fe was mainly

Fig. 4 Spatial distribution patterns of **a** Cl^- , **b** Fe and **c** F^- contents in groundwater samples of the study area



found in the north-eastern part of the study area (Fig. 4b). The rock–water interaction may be the explanation for higher values of Fe in groundwater of the study area. In the Quaternary sediments of the study area, the laterites/lateritic soil and lateritic gravel are present. The interaction

of rain water with the Fe-rich sediments during infiltration was probably the main factor for high Fe content in groundwater. The groundwater at the Fe-rich sites is found to be of unpleasant taste and obnoxious odour like swampy, sewage or rotten vegetation indicating the presence of

organic matter; it seems that organic matter might also have influence on iron enrichment in groundwater of the study area. The detected concentration of Mn is within the desirable limit (0.1 mg/L) at 61.3% sampling sites. The strong significant correlation ($r = 0.762$) of Mn with Fe (Table 4), indicates an origin of Mn like Fe. The Cu content is within the enviable limit (0.05 mg/L) at 96.8% detected sites (Table 3), whereas the Zn concentration was found within the safe limit (5 mg/L) at all detected locations.

Spatial distribution of fluoride

The spatial distribution of F^- in groundwater samples of the study area is shown in Fig. 4c; the F^- concentration recorded at 147 sites, distributed in the 49 villages of the study area is given in Table 6. In the context of health effects of F^- in drinking water, the F^- concentration in the study area is classified into *three categories* (<0.60, 0.60–1.20 and >1.20 mg/L) as shown in Table 6. *First category*—the low concentration of F^- (<0.60 mg/L) was recorded in the greater part of the area (126 samples, 85.71%); the majority of these tube wells were completed in the alluvium zone. The people living in these areas (46 villages) are consuming water with low F^- content. *Second category*—only 9 samples (6.12%) contain F^- in safe range (0.60–1.20 mg/L), and these tube wells are distributed in 7 villages. *Third category*— F^- concentration above 1.20 mg/L was determined in 12 samples (8.16%) mainly in the central part (2 villages, Asanjola and Balia in Narayanpur GP, southern bank of Brahmani River) and north-central part (4 villages, namely Madhabpur, Kanglapahari, Dhabuni and Saldaha in Haridaspur GP, northern bank of Brahmani River) of the study area (Table 6; Fig. 1d). Among these, the tube wells at maximum sites have reached the Rajmahal rocks and water is from the weathered residuum or fracture zone in rocks or intertrappean sediments within a depth range of 45.72–97.54 m. The waters of this category are totally unsafe for drinking and other domestic uses.

The spatial distribution of F^- in the study area is indicating a lithological control on F^- concentration in groundwater. The higher rate of evaporation and longer interaction of water with the aquifer materials under alkaline environment are the key factors for the concentration of F^- (Subba Rao 2009). The weathering of F^- -rich rocks/minerals is the source of F^- in the study area. The F^- -bearing minerals may be also of secondary origin, present in the fracture zone of Rajmahal rocks or intertrappean sediments or weathered residuum. It may be mentioned that Rajmahal basalts form a north–south-trending belt extending over 4100 km² along the eastern

margin of Indian Shield and contain about 28 flows; the intertrappean beds are largely tuffaceous, but include argillaceous (clay, shale) and arenaceous (sand, sandstone, siltstone) units (Ghose et al. 1996).

The overall groundwater is recharged vertically by infiltrating meteoric water and laterally mainly along fractures of Rajmahal rocks, whereas discharge occurred via evaporation and groundwater abstraction. The general groundwater flow is observed from the north-western to south-eastern part of the study area (Fig. 3). The F^- concentration is found to increase along the groundwater flow direction; the spatial variation of F^- concentration along the flow direction is due to the compositional disparity of aquifer rocks, intensity of weathering and residence time of contacts of groundwater with the host rocks. The elevated F^- rich well sites are found to be in the groundwater discharge zones.

In rural areas, the use of chemical fertilizer for agriculture may also contribute F^- in groundwater. But this is probably not true for the present study area because the concentration of PO_4^{3-} is very low and it bears no positive relation with F^- (Table 4) and the samples located in proximity to agricultural fields do not have elevated concentration of F^- compared to domestic wells.

Hydrogeochemistry of fluoride

The F^- shows positive significant correlations with pH, Na^+ , Cl^- , EC and TDS and significant negative correlations with Ca^{2+} , Mg^{2+} and TH (Table 4). The geochemical enrichment of F^- in the study area may be explained using these parameters. From the relations of F^- with pH, Na^+ and Ca^{2+} , it can be interpreted that F^- concentration in groundwater of the study area is primarily associated with geochemical reactions of increasing pH and Na^+ and decreasing Ca^{2+} .

The pH has a significant role in F^- solubility; at a pH range of 5–6.5, F^- solubility is low and the F^- is adsorbed on the surface of the clay (Viero et al. 2009). The higher pH values (>7) of the investigated groundwater samples are supposed to be greater than the *point of zero charge* (PZC) of most minerals (<7–8); in such system, the surface charge of the solids is neutral or slightly negative, which depresses the adsorption of negatively charged F^- (Wei et al. 2015). Conversely, as OH^- and F^- ions have similar ionic radius (0.136 nm), the OH^- in groundwater can replace the exchangeable F^- of clay minerals (biotite/muscovite, illite, chlorite, and amphiboles) resulting in increase of F^- concentration in groundwater (Guo et al. 2007; Singh et al. 2011). The replacement of F^- from biotite and muscovite by OH^- of water can be shown by the equations (Singh et al. 2011), as given below:

Table 6 Villages and fluoride concentration in tube wells of the study area

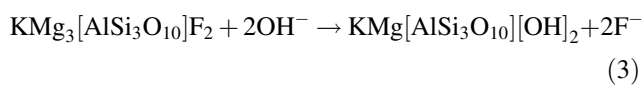
Sl. no.	Village	Sample nos.	Depth of tube wells (m)	F ⁻ concentration (mg/L)			
				Range	<0.60	0.60–1.20	>1.20
				No. of samples			
<i>Narayanpur Gram Panchayat</i>							
1	Kirtipur	1, 2	14.66–18.29	0.20	2	–	–
2	Baidara	3–5	8.64–17.07	0.17–0.18	3	–	–
3	Kusumdoi	6, 7	25.91–26.21	0.18–0.28	2	–	–
4	Turukdighi	8	54.86	0.33	1	–	–
5	Kanaipur	15, 72	28.65–30.48	0.22–0.26	2	–	–
6	Naishorgram	10, 11, 73	17.07–24.38	0.15–0.34	3	–	–
7	Asanjola	12–14, 17, 19, 20	23.17–97.54	0.19–15.6	4	–	2
8	Tetulbadhi	31, 32	23.17	0.19	2	–	–
9	Balia	34–41, 71	19.81–57.91	0.07–5.9	7	–	2
10	Mrityunjoypur	42, 43, 46–49	21.34–54.86	0.17–0.94	5	1	–
11	Indradanga	44, 45	20.12–54.86	0.22–0.23	2	–	–
12	Narayanpur	50–55, 57	13.64–57.91	0.15–0.26	7	–	–
13	Salbani	58, 59	18.29–19.81	0.15–0.22	2	–	–
14	Natunpara	60, 61	54.86–56.39	0.18	2	–	–
15	Khedamara	62–64	57.91–59.44	0.20–0.38	3	–	–
16	Paikpara	65, 66	41.15–51.82	0.16–0.17	2	–	–
17	Upar ranigram	67	56.39	0.13	1	–	–
18	Ranigram	68	14.50	0.19	1	–	–
19	Laldanga	69	53.34	0.73	–	1	–
20	Kharidanga	70	25.91	0.13	1	–	–
<i>Haridaspur Gram Panchayat</i>							
21	Madhabpur	21–30	10.74–54.86	0.15–17	8	–	2
22	Kartikdanga	74–78	12.95–18.29	0.023–0.23	5	–	–
23	Bildanga	79, 80	14.28–27.43	0.058–0.12	2	–	–
24	Kayerbil	81	21.34	0.12	1	–	–
25	Santoshpur	82, 83	21.34–45.72	0.12–0.29	2	–	–
26	Kalurpukur	84, 85	54.86–60.96	0.058–0.072	2	–	–
27	Jamsol	86	68.58	0.16	1	–	–
28	Udaynagar	87, 97	24.38–27.43	0.066–0.25	2	–	–
29	Haridaspur	88, 100, 101	27.43	0.098–0.18	3	–	–
30	Lakhijol	90	14.02	0.056	1	–	–
31	Joypur	91–96	18.28–45.72	0.15–0.27	5	1	–
32	Kamarpara	99	27.43	0.6	–	1	–
33	Alampur	102–105	18.29–51.82	0.12–0.26	4	–	–
34	Lakhinarayanpur	106–114	19.51–73.15	0.03–1	7	2	–
35	Kanglapahari	115–120	64.01–67.06	0.058–8	3	–	3
36	Asanbani	121, 122	54.86	0.16–0.18	2	–	–
37	Dhabuni	123–127	60.96–67.06	0.13–19	2	1	2
38	Saldaha	128–131	54.86–57.91	0.22–18	1	2	1
39	Dadupara	132	64.01	0.23	1	–	–
40	Singhadohori	133, 135, 136	27.43	0.21–0.26	3	–	–
41	Jungul	137, 138	25.91–27.43	0.17–0.20	2	–	–
42	Tarapur	139, 140	17.37–70.10	0.20–0.23	2	–	–
43	Bherapara	141	19.86	0.16	1	–	–
44	Nasipur	142	10.67	0.10	1	–	–

Table 6 continued

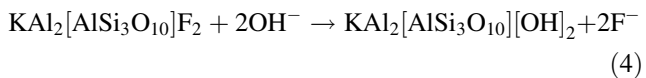
Sl. no.	Village	Sample nos.	Depth of tube wells (m)	F ⁻ concentration (mg/L)			
				Range	<0.60	0.60–1.20	>1.20
				No. of samples			
45	Balarampur	143, 144	16.15–18.29	0.11–0.18	2	–	–
46	Dastarpur	145–148	27.43–28.96	0.19–0.22	4	–	–
47	Guniha	149–151	21.34–27.43	0.16–0.27	3	–	–
48	Bhagabatipur	152–154	18.28–21.34	0.15–0.22	3	–	–
49	Bajpara	155	21.34	0.35	1	–	–
Total samples		147	8.64–97.54	0.023–19	126 (85.71%)	9 (6.12%)	12 (8.16%)

Villages (in bold): F⁻ concentration >1.20 mg/L, total six villages in the study area

Biotite



Muscovite



In the present area, the alkaline conditions (pH 6.67–9.98) may have favoured the leaching of F⁻ in groundwater at some places; the significant and positive correlation of pH with F⁻ (*r* = 0.441) supports this fact (Table 4). The question may come for other sites of the study area where F⁻ concentrations are low although pH values are high. This may be due to the different composition of aquifer materials that have insufficient amount of F⁻ containing mineral or owing to the short period of rock-water interactions. It may be mentioned that in the study area, the TDS (or EC) values of majority samples are low in comparison to the samples with elevated F⁻ concentrations.

The enrichment of F⁻ in groundwater may also be associated to ion exchange; during ion exchange process, Ca²⁺ in water is exchanged with Na⁺ in aquifer matrixes due to the slow movement of groundwater. This condition does not allow formation of CaF₂ to precipitate but increases the solubility of F⁻ containing minerals due to the increase in Na⁺ concentration in the solution. In the present study, the significant positive correlation of F⁻ with Na⁺ (*r* = 0.707) and significant negative correlation with Ca²⁺ (*r* = -0.666) indicate that the mobility of F⁻ has been influenced by the ion exchange process.

The ionic ratios of Na⁺/Ca²⁺ and HCO₃⁻/Ca²⁺ are found much greater than 1 in the F⁻ contaminated groundwaters, revealing the favourable conditions for F⁻ dissolution process and low calcium activity, respectively in the study area (Fig. 5a, b). The high Na⁺/Ca²⁺ ratio means that Na⁺ has

increased and/or Ca²⁺ has decreased through reverse ion exchange process and/or calcite precipitation; the high HCO₃⁻/Ca²⁺ ratio also indicates the low Ca²⁺ concentration in water and precipitation of calcite.

TDS and EC values are high in F⁻ contaminated waters and also show a significant positive relation with F⁻ (Table 4). These apparently mean that the elevated F⁻ concentration in groundwater (Group 3, Table 6) is related to the key hydrochemical processes that control groundwater chemistry in the study area. It is already mentioned that F⁻ has a significant negative relation with Ca²⁺ and Mg²⁺; F⁻ also shows a negative relation with HCO₃⁻ (*r* = -0.354), though statistically not significant. These imply that most probably the F⁻ and the three ions namely Ca²⁺, Mg²⁺ and HCO₃⁻ are not from the dissolution of the same silicate mineral containing F⁻.

The dry climate may have also role in F⁻ enrichment; the temperature increases the solubility and rate of dissolution of minerals (Hem 1985). The findings of laterite and lateritic soil in the study area indicate the influence of evaporation process in precipitation of calcite (CaCO₃). The plots of saturation indices (SI) of calcite and fluorite for groundwater samples of the study area are presented in Fig. 5c. The dashed lines indicate the approximate boundaries of equilibrium zone with an extent of ±0.5 units to consider the errors related to field and analytical measurements involved in working out of SI. The figure shows that majority of the samples (61.29%) are oversaturated with respect to calcite (CaCO₃); among the remaining, 22.58% samples are in equilibrium state and the rest (16.13%) are under saturated. In respect of fluorite (CaF₂), the greater part of the samples (83.87%) is under saturated and the rest of the samples (sample nos. 13, 21, 36, 117, 120) are either in the equilibrium range or approaching equilibrium. These samples are F⁻ contaminated groundwater and are also oversaturated or in equilibrium range with regard to CaCO₃. The oversaturation in

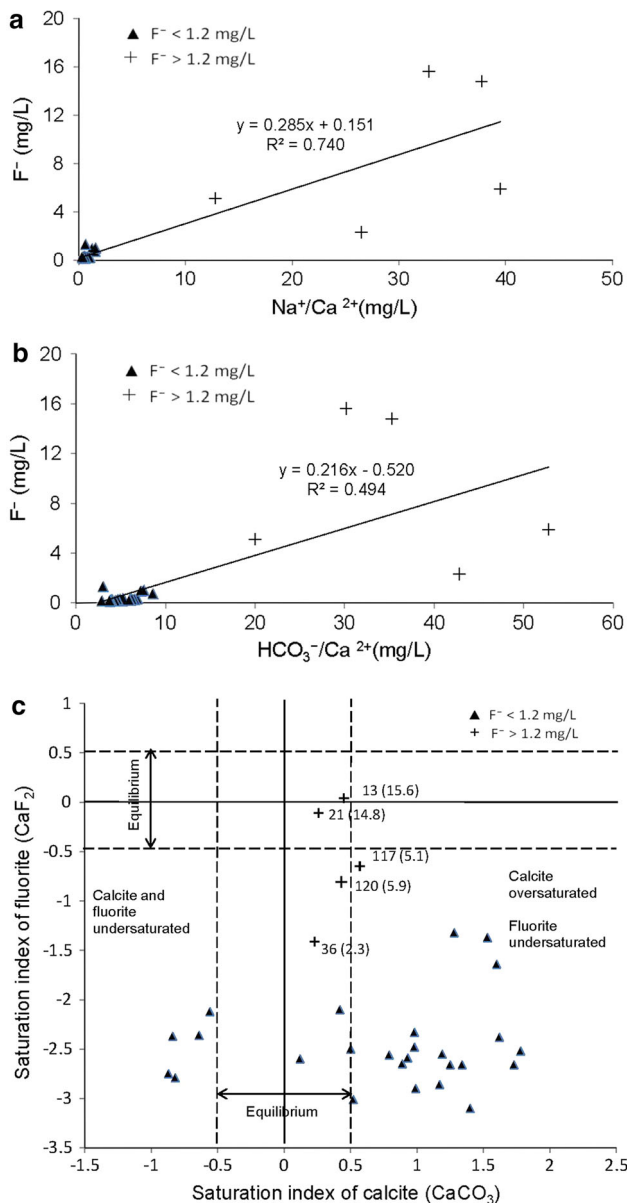


Fig. 5 **a** F^- versus Na^+/Ca^{2+} , **b** F^- versus HCO_3^-/Ca^{2+} and **c** Calcite saturation index versus fluorite saturation index

respect of a mineral reveals the abundance of that mineral in the host rock and long period of rock–water interaction.

From the above observations, it appears that the concentrations of Ca^{2+} and F^- in groundwater of the F^- rich sites of the study area are controlled by the CaF_2 solubility, $K_{fluorite} = 10^{-10.6}$ (Chae et al. 2007). In line with present results, earlier studies have demonstrated that groundwaters containing elevated F^- concentrations are often in equilibrium with calcite; the equilibrium relationship between F^- and Ca^{2+} is constrained by CaF_2 as given in Eq. 5 in the logarithmic form (Hu et al. 2013):

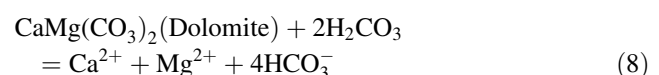
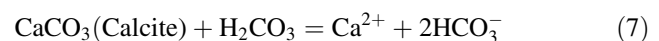
$$\log K_{CaF_2} = \log[Ca^{2+}] + 2 \log[F^-] \quad (5)$$

After oversaturation, the concentration of Ca^{2+} ions overrides the solubility limit of CaF_2 , as CaF_2 dissolution is suppressed by a common ion effect. The occurrence of this situation gave a negative relation of F^- with Ca^{2+} (Handa 1975; Apambire et al. 1997; Guo et al. 2007). The oversaturation of $CaCO_3$ due to evaporation and subsequently precipitation of $CaCO_3$ have created a deficiency of Ca^{2+} ions in groundwater of the study area; ion exchange process has also played a role in the dearth of Ca^{2+} ions.

Groundwater type and fluoride concentration

Chemical data of 31 groundwater samples from the study area were plotted on the Piper diagram (Fig. 6). The classification of hydrochemical facies is based on major cation and anion percentages and water type is according to subdivisions of the diamond field (Back 1966). The water type and hydrochemical facies at different locations are given in Table 7. The study reveals that majority of the samples (83.9%) belong to $CaHCO_3$ type followed by mixed $NaHCO_3$ (9.7%) and $NaCl$ (6.4%) types. The plots on Piper diagram also indicate that alkaline earths (Ca^{2+} and Mg^{2+}) and weak acid (HCO_3^-) exceed over alkalis (Na^+ and K^+) and strong acids (SO_4^{2-} and Cl^-), respectively at majority of the locations (90.32%). Among the total 13 hydrochemical facies, 11 facies (83.9% samples) fall under the $CaHCO_3$ water type; one facies falls under $NaHCO_3$ type and another one under $NaCl$ type (Fig. 6; Table 7).

If grouping of waters based on F^- concentration (Table 6) is considered, it is seen that water samples of Group 1 ($F^- < 0.60$ mg/L) and Group 2 ($F^- = 0.60$ – 1.20 mg/L) are of $CaHCO_3$ water type; in these waters, the Ca^{2+} and Mg^{2+} are dominant cations, while HCO_3^- is the predominant anion. They are typically recharge water derived in a geological environment containing carbonate minerals like calcite and dolomite and suggest the geochemical implication of gas P_{CO_2} as a controlling factor. The infiltrating meteoric water gets enriched in CO_2 from soil, air and biochemical reactions and afterwards CO_2 in reaction with water forms carbonic acid (Eq. 6); subsequently, the Ca, Mg and HCO_3^- are derived through the interactions of carbonic acid with calcite and dolomite (Eqs. 7, 8), as explained below:



The Ca^{2+} , Mg^{2+} and HCO_3^- may also be derived from the dissolution of silicate minerals. A general reaction for the

Fig. 6 Piper diagram showing the major ion composition and groundwater types. F⁻-contaminated water samples (F⁻ > 1.2 mg/L) are indicated

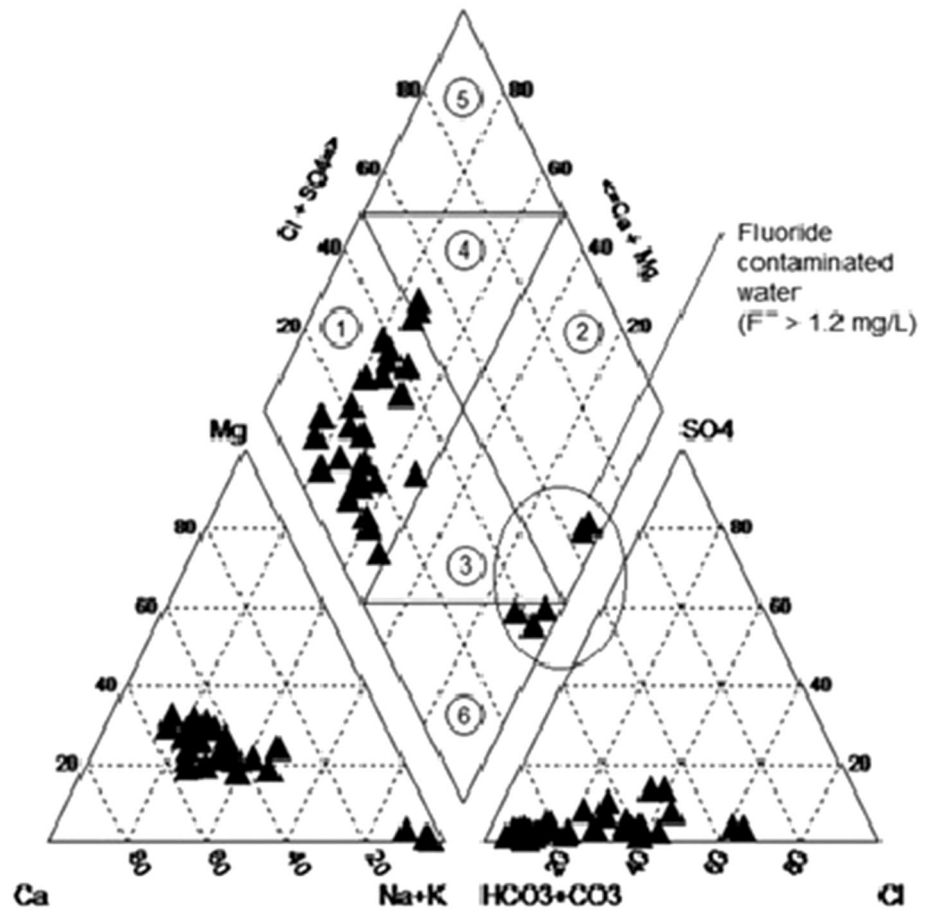
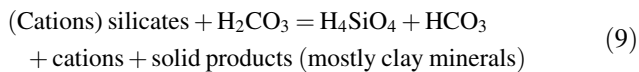


Table 7 Summary of hydrochemical facies

Sl. no.	Facies	Sample nos. (number of samples)	Percentage of samples	Sl. no.	Facies	Sample nos. (number of samples)	Percentage of samples
I	Ca–Mg–HCO ₃	6, 8, 61, 72 (4)	12.9	VIII	Ca–Mg–HCO ₃ –Cl	138, 149 (2)	6.45
II	Ca–Na–HCO ₃	136 (1)	3.22	IX	Ca–Na–HCO ₃ –Cl	28, 34 (2)	6.45
III	Na–Ca–HCO ₃	69 (1)	3.22	X	Na–Ca–Mg–HCO ₃	48 (1)	3.22
IV	Na–Cl–HCO ₃	13, 21 (2)	6.45	XI	Ca–Mg–Na–HCO ₃ –Cl	66, 123, 129, 144 (4)	12.9
V	Na–HCO ₃ –Cl	36, 117, 120 (3)	9.7	XII	Ca–Na–Mg–HCO ₃ –Cl	103, 152 (2)	6.45
VI	Ca–Mg–Na–HCO ₃	10, 14, 74, 91(4)	12.9	XIII	Na–Ca–Mg–HCO ₃ –Cl	107 (1)	3.22
VII	Ca–Na–Mg–HCO ₃	1, 43, 58, 83 (4)	12.9				

With reference to diamond field of Piper diagram (Fig. 6)—facies I–III, VI–XIII fall in area 1 (CaHCO₃ type, 26 samples, 83.9%); facies V fall in area 6 (NaHCO₃ type, 3 samples; 9.7%); facies IV fall in area 2 (NaCl type, 2 samples, 6.4%)

weathering of silicate rocks with carbonic acid is as follows (Eq. 9):

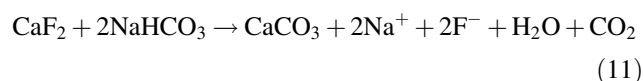
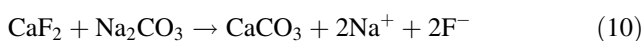


The Group 3 waters ($\text{F}^- > 1.20 \text{ mg/L}$) are mainly of NaHCO_3 type (ion association $\text{Na-HCO}_3\text{-Cl}$); two samples (nos. 13, 21) of Group 3 are of NaCl type (ion association: Na-Cl-HCO_3) (Table 7). The distribution pattern of these waters in Piper diagram (Fig. 6) suggests a chemical evolution through contemporaneous processes of interaction with silicate rocks, ion exchange and evapotranspiration. Finally, the composition of water is influenced by the infiltration of waste water.

As CaHCO_3 -type water travels through the rocks, its chemical composition changes. Usually, the longer the residence time that water remains in contact with the aquifer rocks, the greater the amount of material into solution. Water composition also alters with increasing depth of journey, as bicarbonate anions give ways to accommodate anions like sulphate and chloride. NaHCO_3 type of groundwater (F^- rich and Ca^{2+} poor) is mainly a result of ion exchange reaction and precipitation of carbonates as secondary minerals at high alkaline conditions (Jacks et al. 2005). The Na^+ adsorbed on the clay surface is replaced by Ca^{2+} in solution. A portion of Na^+ in groundwater also may have derived by the weathering of plagioclase feldspars. The NaCl type of water originally was of the NaHCO_3 type; because of excess Cl^- , originated from the mixing of waste water in groundwater, the ion association has changed as Na-Cl-HCO_3 and samples plotted in the area of NaCl type of water of Piper diagram (Fig. 6). In the present study area, the hydrogeochemical evolution shows a path from CaHCO_3 type via NaHCO_3 to NaCl type.

Based on F^- concentration, the major water types in the study area may be arranged as, $\text{NaHCO}_3 > \text{CaHCO}_3$. This indicates that the excess aqueous ionic concentration of NaHCO_3 in groundwater has influence on the fluorite solubility behaviour; the excess NaHCO_3 activates the processes of dissociation and dissolution of F^- from the fluorite (CaF_2) mineral.

Previous works also reported that NaHCO_3 type of water is proficient for dissolution of fluorite (CaF_2) mineral (Jacks et al. 2005; Chae et al. 2007; Guo et al. 2007); the CaF_2 dissolution process may be expressed by the following equations (Singh and Mukherjee 2015):



Hydrogeochemical processes

The $\text{Ca}^{2+} + \text{Mg}^{2+}$ versus $\text{HCO}_3^- + \text{SO}_4^{2-}$ scatter diagram (Fig. 7a) shows that greater part of the samples plunge below the 1:1 equiline, indicative of silicate weathering; few points plot above the equiline revealing carbonate weathering, whereas samples plot along the equiline suggesting weathering of both carbonates and silicates (Rajmohan and Elango 2004; Kumar et al. 2006). The relationship between $\text{Na}^+ + \text{K}^+$ and total cations (TZ^+) reveals that the samples are plotted well below the $\text{Na}^+ + \text{K}^+ = 0.5\text{TZ}^+$ line (Fig. 7b) with an equilibrium ratio of 0.15–0.96 (mean 0.39, median 0.30) indicating the involvement of silicate weathering in the geochemical processes (Stallard and Edmond 1983), which contributes mainly Na^+ and K^+ ions to the groundwater at majority locations of the study area. The plots of $\text{Ca}^{2+} + \text{Mg}^{2+}$ versus total cations (TZ^+) of groundwater samples (Fig. 7c) also lie below the 1:1 equiline indicating that some of these ions (Ca^{2+} , Mg^{2+}) resulted from the weathering of silicate minerals; the equilibrium ratio of ($\text{Ca}^{2+} + \text{Mg}^{2+}$) with (TZ^+) ranging from 0.04 to 0.85 (mean 0.61, median 0.70) reveals that alkaline earths are enriched 2–2.5 times the amount of alkalis.

Changes in chemical composition of groundwater along its flow path due to ion exchange can be understood by studying the Chloro-Alkaline Indices (CAI). Schoeller (1965, 1967) proposed two indices (CAI-1 and CAI-2) for the interpretation of ion exchange between groundwater and host environment. The computation of the indices (CAI-1 and CAI-2) was performed using the following equations:

$$\text{CAI-1} = [\text{Cl}^- - (\text{Na}^+ + \text{K}^+)]/\text{Cl}^- \quad (12)$$

$$\begin{aligned} \text{CAI-2} = &[\text{Cl}^- - (\text{Na}^+ + \text{K}^+)]/(\text{SO}_4^{2-} + \text{HCO}_3^- + \text{CO}_3^{2-} \\ &+ \text{NO}_3^-) \quad (\text{all values are in meq/L}). \end{aligned} \quad (13)$$

If Na^+ and K^+ in water are exchanged with Mg^{2+} and Ca^{2+} of the rock, both the indices are found to be positive. The reverse case is indirect exchange where the CAI values are expected to be negative. About 74.2% of the groundwater samples of the study area indicate negative values for both indices (Fig. 8a) suggesting the dominance of reverse ion exchange that has increased Na^+ and K^+ in the groundwater. The indices of the groundwater vary from -4.47 to 0.48 and -1.17 to 0.33 for CAI-1 and CAI-2, respectively. The larger the absolute values of indices, the greater the impact of cation exchange on groundwater chemistry which may be reflected through high $\text{Na}^+/\text{Ca}^{2+}$ ratios and Na^+ contents; this is observed particularly with

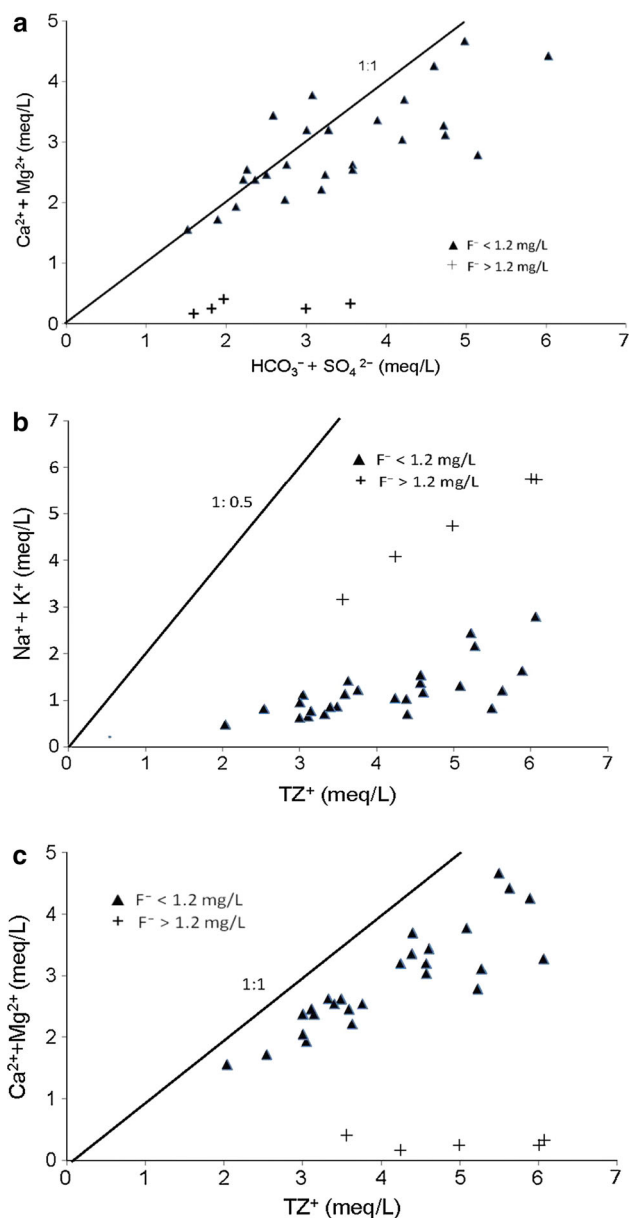


Fig. 7 Plots of **a** $\text{Ca}^{2+} + \text{Mg}^{2+}$ versus $\text{HCO}_3^- + \text{SO}_4^{2-}$, **b** $\text{Na}^+ + \text{K}^+$ versus total cation (TZ^+) and **c** $\text{Ca}^{2+} + \text{Mg}^{2+}$ versus total cation (TZ^+)

respect to some F^- -rich groundwater samples in the study area. 28.5% of samples exhibited positive values of indices; these samples, relatively with higher Ca^{2+} and Mg^{2+} concentrations, indicate the recharge and flow-through zones.

The occurrence of cation exchange reaction in groundwater can also be evidenced from a linear plot between $[(\text{Ca}^{2+} + \text{Mg}^{2+}) - (\text{HCO}_3^- + \text{SO}_4^{2-})]$ (meq/L) and $[(\text{Na}^+ + \text{K}^+) - \text{Cl}^-]$ (meq/L); these two indices provide clues on the contribution of cation exchange to the balance of the alkali and alkaline earth elements (Wen et al. 2005; Kortatsi 2007). The $[(\text{Na}^+ + \text{K}^+) - \text{Cl}^-]$ represents contribution from sources other than the dissolution of

chlorides to the concentrations of Na^+ and K^+ in groundwater, whereas $[(\text{Ca}^{2+} + \text{Mg}^{2+}) - (\text{HCO}_3^- + \text{SO}_4^{2-})]$ represents the contribution of the main alkaline earth elements from sources other than the dissolution of the sulphates and carbonates of these elements. If cation exchange is not a significant reaction in the aquifer system, all data will plot close to the origin; but where cation exchange has important contribution in groundwater composition, the data will plot along a line with a slope of nearly -1 .

In the current study (Fig. 8b), majority of the samples fall along a line with a slope of -1.074 and away from the origin of the X-axis indicating that ion exchange has significant role in the concentration of Na^+ , Ca^{2+} and Mg^{2+} in groundwater. In the study area, $\text{Na}^+/\text{Ca}^{2+}$ equivalent ratios for the F^- rich samples ranges within 11.15–34.45; these variations are found to have no association with the changes in total cation (TZ^+)/ Cl^- equivalent ratios (Table 2). This is due to the ion exchange between Ca^{2+}

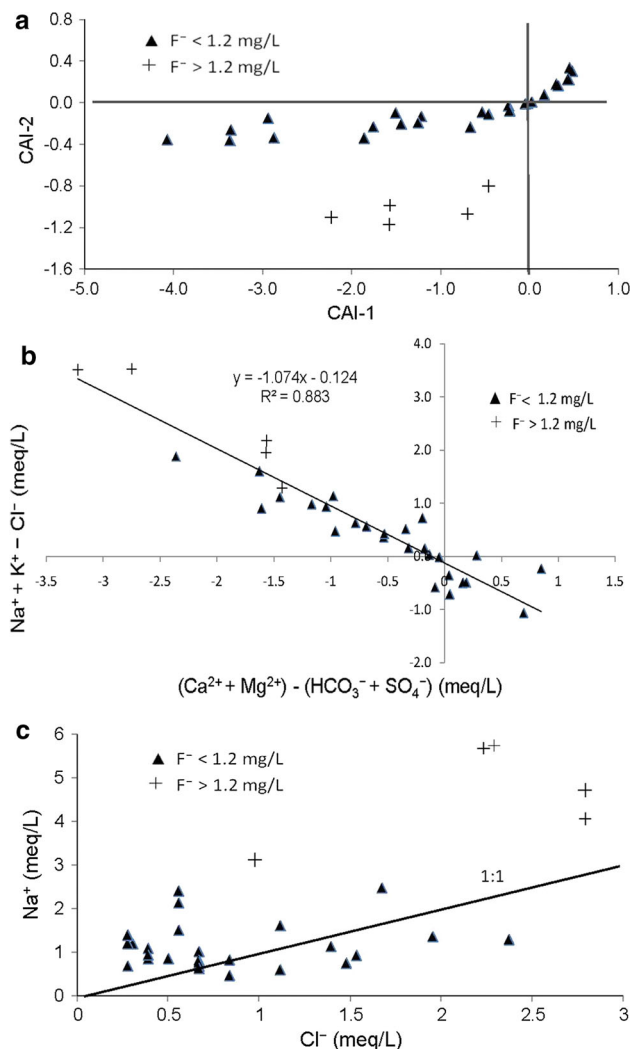
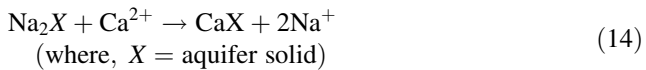


Fig. 8 Plots of **a** CAI-1 versus CAI-2, **b** $(\text{Na}^+ + \text{K}^+) - \text{Cl}^-$ versus $(\text{Ca}^{2+} + \text{Mg}^{2+}) - (\text{HCO}_3^- + \text{SO}_4^{2-})$ and **c** Na^+ versus Cl^-

from groundwater and Na^+ on clay surfaces (Eq. 14), rather than progressive dissolution of Na^+ -bearing minerals (e.g. albite) (Mondal et al. 2014).



The evapotranspiration of groundwater in its pathway due to the semi-arid climate of the study area has also influence in the precipitation of CaCO_3 and mobilization of F^- in groundwater.

The high concentration of Cl^- reveals a long period of residence of groundwater in the (1) zone of stagnation and/or slow movement of groundwater and (2) groundwater trough (Sikdar and Chakraborty 2008). The excess Cl^- in groundwater is mainly a phenomenon of dissolution of halite or anthropogenic impacts. If halite is responsible for the Na^+ and Cl^- ions in groundwater, the Na^+/Cl^- molar ratio will be approximately 1 as the halite mineral is composed of equal molar fractions of Na^+ and Cl^- ions, whereas a ratio greater than 1 may be interpreted as Na^+ released from silicate weathering (Meybeck 1987; Deutsch 1997). The excess Na^+ can also be attributed to anthropogenic activities like waste water. Usually wastewater is enriched in Na^+ relative to Cl^- (Vengosh and Keren 1996). The significant positive correlation of Na^+ with Cl^- ($r = 0.673$) indicates that waste waters may have also contributed some amount of Na^+ in groundwater of the present study area. The possible sources of excess Cl^- in groundwater are sea water, urban and municipal sources like road deicers, municipal landfills, rural sources such as septic effluents, animal waste, chemical fertilizer, and polluted ponds (Batabyal and Chakraborty 2015). These sources can result in significant concentrations of Cl^- in groundwater because chloride is readily transported through the soil (Stallard and Edmond 1983). The present study area is in continental set-up and the sea is far away. Moreover, the molar ratio of Na^+/Cl^- for maximum groundwater samples is above 1 (range 0.50–4.95). The scatter plot of Na^+ versus Cl^- (Fig. 8c) shows that the greater part of the groundwater samples lie above the equiline, indicating major control by silicate weathering. These facts confirm that the excess Cl^- is not due to the influence of marine water rather some anthropogenic factors are responsible. The urban or municipal activities, as mentioned above, are not prevailing in the present study area. Most probably, the infiltration of waste water is the prime cause of Cl^- contamination in groundwater of the study area. The Cl^- in the wastewater, ranges between 30 and 300 mg/L (McArthur et al. 2012). The waste water may be from domestic/septic tanks, improper sanitary system, polluted ponds and animal wastes; the analysis of nine pond water samples from the study area also shows the high concentration of Cl^- (19.6–181.24 mg/L).

Spatial groundwater association

The groundwater of the study area is classified into three broad clusters (Cluster-1, Cluster-2, and Cluster-3) based on the dendrogram (Fig. 9). The hydrochemical characteristics (Table 8) of the clusters are abridged as follows:

Cluster-1 CaHCO_3 type, represents recharge waters with short residence times; the water of this cluster is found at greater part of the study area as evidenced from 48.4% of samples. The groundwater is alkaline (mean pH 8.44) and moderately hard (mean TH 119.31) with lowest EC (mean 288.13 $\mu\text{S}/\text{cm}$) and TDS (mean 204.47 mg/L) among the three clusters. F^- concentration is very low (mean 0.22 mg/L), whereas Fe content is high (mean 3.44 mg/L). Cl^- concentration (mean 22.10 mg/L) is high and may be attributed to anthropogenic inputs as discussed in an earlier section. The water is fresh and primarily is a result of dissolution of carbonate minerals. The water of this cluster can be used for drinking and domestic uses after standard treatments in order to diminish the elevated Fe concentration; enhancement of F^- concentration to a drinking range (0.60–1.20 mg/L) would be beneficial for the health of teeth and bones.

Cluster-2 This is also CaHCO_3 type of water found at 35.5% sampling points. F^- concentration ranges from 0.14 to 1 mg/L (mean value 0.41 mg/L). The Fe and Cl^- contents are high (mean values 1.59 mg/L and 41.30 mg/L).

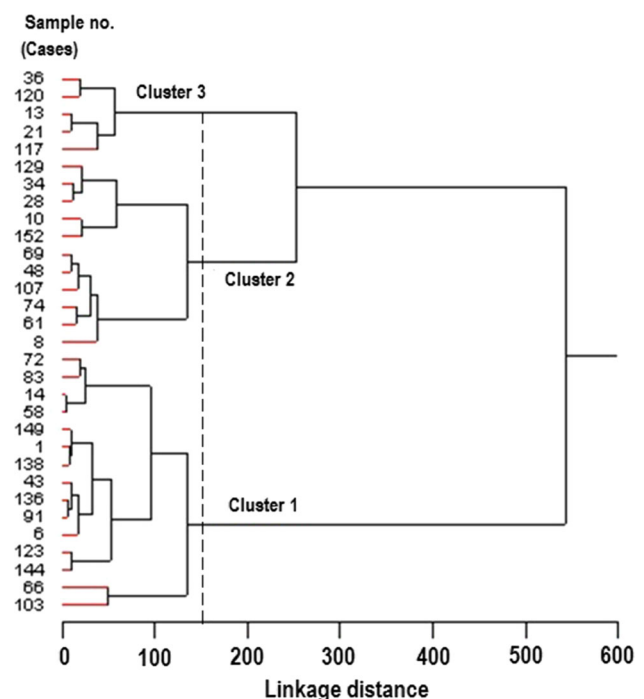


Fig. 9 Dendrogram resulting from Q-mode hierarchical cluster analysis (dotted line denotes “phenon line” drawn by the investigator to select the number of clusters)

Table 8 Chemical constituents of three clusters

Cluster type	Cluster 1		Cluster 2		Cluster 3	
Sample nos.	72, 83, 14, 58, 149, 1, 138, 43, 136, 91, 6, 123, 144, 66, 103 (48.4% of samples)		129, 34, 28, 10, 152, 69, 48, 107, 74, 61, 8 (35.5% of samples)		36, 120, 13, 21, 117 (16.1% of samples)	
Parameter	Range	Mean	Range	Mean	Range	Mean
pH	6.84–9.6	8.44	6.67–9.5	8.53	8.71–9.98	9.45
EC	201–350	288.13	409–535	468.45	456–577	532.2
TDS	140–250	204.47	290–377	333.91	320–415	365.6
TA	71.4–204	132.60	102–295.8	199.36	71.4–173.4	112.2
TH	34.61–185.4	119.31	140.1–234.84	180.54	8.24–24.72	14.83
SiO ₂	33.12–96.7	47.96	34.04–68.72	52.03	22.92–45.34	34.46
Na ⁺	10.52–34.4	20.14	18.54–56.7	34.01	71.6–130.85	106.87
K ⁺	<1–11.1	2.52	<1–12.7	3.49	<1–3.4	2.03
Ca ²⁺	21.42–48	31.18	36.26–57.68	45.99	2.47–5.6	3.92
Mg ²⁺	5.93–15.82	10.42	10.88–21.75	15.73	0.5–1.5	1
Cl ⁻	9.9–52.43	22.10	10.89–84.12	41.30	34.64–99	78.19
F ⁻	0.13–0.29	0.22	0.14–1	0.41	2.3–15.6	8.74
SO ₄ ²⁻	4–25.27	8.37	2.26–26.34	9.65	4.07–8.85	6.8
HCO ₃ ⁻	87.11–248.88	161.77	124.44–360.88	243.23	87.11–211.55	136.88
Fe	<0.05–29.84	3.44	0.07–12	1.59	0.09–0.69	0.28

pH in numeric units, EC in $\mu\text{S}/\text{cm}$, all other parameters in mg/L ; the range of F^- is based on 31 groundwater samples, considered for detail chemical analysis

L, respectively) like Cluster-1. The basic difference with Cluster-1 is that the water of Cluster-2 shows higher values with respect to EC, TDS, HCO_3^- and TH. This is also fresh water and evolution is very much similar to water of Cluster-1. This water may also be consumed after proper treatments for reduction of Fe concentration and hardness.

Cluster-3 Two water types, NaHCO_3 (sample nos. 36, 117, 120) and NaCl (sample nos. 13, 21) are identified in this cluster. The groundwater of Cluster-3 is highly alkaline (mean pH 9.45), moderately mineralized (mean EC 532.2 $\mu\text{S}/\text{cm}$, mean TDS 365.6 mg/L) and soft (mean TH 14.83); EC and TDS values are highest and TH value is lowest among the three clusters. The water of the cluster shows elevated F^- concentration (2.3–15.6 mg/L), very low Ca^{2+} (mean 3.92 mg/L) and Mg^{2+} (mean 1 mg/L) and high Na^+ (mean 106.87 mg/L) contents. The EC and TDS values indicate that the groundwater had moved a longer path and thus had a longer residence time of rock–water interaction which facilitated additional enrichment of the available ions including F^- along the flow passage. The water of this cluster contains Fe (mean 0.28 mg/L) within the desirable limit. Owing to the high concentration of F^- , the water of this cluster is not suitable for drinking; consumption of this water will pose dental and skeletal fluorosis. This type of water is found in the six villages of study area as mentioned in the earlier section (Fig. 1d; Table 6).

Conclusions

The hydrogeochemical investigation has revealed that the water is alkaline, soft to hard with low to moderate mineralization. At majority places, SiO_2 , Fe and Cl^- contents are recorded high; the elevated SiO_2 may be due to the weathering of host rocks rich in SiO_2 and mixing of air borne silica. The interactions of the infiltrating water with laterites and lateritic soil have enriched the Fe content under reducing state, whereas the excess Cl^- is due to the mixing of domestic waste water in groundwater.

The F^- concentration varies from 0.023 to 19 mg/L (based on 147 samples) and spatial distribution pattern indicates a lithological control on its enrichment in groundwater; the high concentration of F^- (>1.20 mg/L) is mainly detected in water samples from the weathered residuum or fracture zone or intertrappean sediments of Rajmahal rocks. Chemical weathering and dissolution of silicates and carbonates and the reverse ion exchange reactions are found to be the key controlling processes for major ions in groundwater. The study reveals that excess F^- originates from the weathering and dissolution of minerals containing F^- promoted by the cation exchange of Na^+ and K^+ in the aquifer substrate against Ca^{2+} and Mg^{2+} in the interacting water; the precipitation of CaCO_3 has made the pathways for dissolution of CaF_2 that in turn has enriched the F^- in groundwater. Possibly, the enrichment of F^- has

also occurred by the exchange of OH^- for F^- on clay minerals at favourable alkaline conditions.

CaHCO_3 is the primary and dominant water type from which the NaHCO_3 and NaCl types are formed; this reveals that the groundwater chemistry is controlled by rock-water interaction and anthropogenic pollution. Among the three spatial clusters, the waters of Cluster-1 and Cluster-2 are CaHCO_3 type; F^- concentration of Cluster-1 is low (<0.60 mg/L) and that of Cluster-2 from low (<0.60) to a value in the safe range (0.60–1.20 mg/L). These waters are suitable for drinking excepting the elevated Fe contents; the low concentration of F^- (<0.60 mg/L) may restrain the proper development of teeth. The Cluster-3 represents F^- -rich (>1.20 mg/L) NaHCO_3 and NaCl types of waters with low Ca^{2+} and Mg^{2+} and high Na^+ ; EC and TDS values are highest and TH value is the lowest among the three clusters. The water is highly unsafe for drinking due to the excess F^- concentration; alternative arrangement like treatment of water adopting a suitable defluoridation technique or tapping of water from shallow alluvium aquifers or rain water harvesting or supply of clean water through pipeline from the river beds may solve the potable water crisis in the F^- affected villages.

Acknowledgements The author is grateful to the Director, CSIR—Central Mechanical Engineering Research Institute, Durgapur, for giving permission to publish this paper. The author is also indebted to CSIR, Govt. of India for the financial support through Clean Water Project (ESC0306). The author acknowledges Ms. Ankita Mukherjee for assistance in the field work. Thanks are due to the Assistant Engineers of Nalhati-I and Rampurhat-I Subdivisions, PHED for providing drilling well log data of Nalhati–Rampurhat areas. The author is also thankful to the Block Development Offices of Nalhati-I and Rampurhat-I and Gram Panchayats of Haridaspur and Narayanpur for providing relevant data and support during the field work.

References

- Apambire WB, Boyle DR, Michel FA (1997) Geochemistry, genesis and health implication of fluoriferous groundwater in the upper regions, Ghana. *Environ Geol* 33:13–24
- APHA (2005) Standard methods for the examination of water and wastewater, 21st edn. American Public Health Association, Washington
- Appelo CAJ, Postma D (2005) Geochemistry, groundwater and pollution, 2nd edn. A A Balkema, Amsterdam
- Back W (1966) Hydrochemical faciès and groundwater flow patterns in northern part of Atlantic coastal plain. US Geological Survey Professional Paper 498-C
- Bardsen A, Bgorraton K, Selving KA (1996) Variability in fluoride content of sub-surface water reservoir. *Acta Odontol Scand* 54:343–347
- Batabyal AK, Chakraborty S (2015) Hydrogeochemistry and water quality index in the assessment of groundwater quality for drinking uses. *Water Environ Res* 87:607–617
- BIS (Bureau of Indian Standards) (1991) Drinking water specification. BIS 10500, pp 1–8
- Central Ground Water Board (1985) Hydrogeology and groundwater resources of Birbhum district, West Bengal. Technical report; series D; no. 30
- Chae GT, Yun ST, Mayer B, Kim KH, Kim SY, Kwon JS, Kim K, Koh YK (2007) Fluorine geochemistry in bedrock groundwater of South Korea. *Sci Total Environ* 385:272–283
- Davis NS (1964) Silica in streams and groundwater. *Am J Sci* 262:870–891
- Davis SN, DeWiest RJM (1966) Hydrogeology. Wiley, New York
- Deutsch WJ (1997) Groundwater geochemistry: fundamentals and applications to contamination. Lewis, New York
- Dobrzynski D (2005) Silica origin and solubility in groundwater from the weathered zone of sedimentary rocks of the Intra-Sudetic Basin, SW Poland. *Acta Geol Pol* 4:445–462
- Freeze AR, Cherry JA (1979) Groundwater. Prentice-Hall, Englewood Cliffs
- Gaciri SJ, Davies TC (1993) The occurrence and geochemistry of fluoride in some natural waters of Kenya. *J Hydrol* 143:395–412
- Ghose NC, Singh SP, Singh RN, Mukherjee D (1996) Flow stratigraphy of selected sections of the Rajmahal basalts, eastern India. *J Southeast Asian Earth Sci* 13:83–93
- Guo Q, Wang Q, Ma T et al (2007) Geochemical processes controlling the elevated fluoride concentrations in groundwaters of the Taiyuan Basin, Northern China. *J Geochem Explor* 93:1–12
- Gupta S, Banerjee S, Saha RN et al (2006) Fluoride geochemistry of groundwater in Birbhum, West Bengal, India. *Fluoride* 39:318–320
- Handa BK (1975) Geochemistry and genesis of fluoride containing groundwaters in India. *Ground Water* 13:275–281
- Handa BK (1988) Fluoride occurrence in natural waters in India and its significance. *Bhu Jal News* 3(2):31–37
- Hem JD (1985) Study and interpretation of the chemical characteristics of natural water, 3rd edn. US Geological Survey Water-Supply Paper 2254
<http://birbhum.gov.in/geog1.htm>. Accessed on 05 Mar 2015
http://cgwb.gov.in/District_Profile/WestBengal/Birbhum.pdf. Accessed on 06 Mar 2015
http://data.gov.in/catalog/villagetown-wise-primary-census-abstract-2011-west-bengal#web_catalog_tabs_block_10. Accessed on 24 July 2015
- Hu S, Luo T, Jing C (2013) Principal component analysis of fluoride geochemistry of groundwater in Shanxi and Inner Mongolia, China. *J Geochem Explor* 135:124–129
- ISI (1983) Indian standard specification for drinking water. IS:10500
- Jacks G, Bhattacharya P, Chaudhary V, Singh KP (2005) Controls on the genesis of some high-fluoride groundwaters in India. *Appl Geochem* 20:221–228
- Jain CK, Bandyopadhyay A, Bhadra A (2010) Assessment of ground water quality for drinking purpose, District Nainital, Uttarakhand, India. *Environ Monit Assess* 166:663–676
- Kortatsi BK (2007) Hydrochemical framework of groundwater in the Ankobra Basin, Ghana. *Aquat Geochem* 13:41–74
- Kumar M, Ramanathan AL, Rao MS, Kumar B (2006) Identification and evaluation of hydrogeochemical processes in the groundwater environment of Delhi, India. *Environ Geol* 50:1025–1039
- McArthur JM, Sikdar PK, Nath B, Grassineau N, Marshall JD, Banerjee DM (2012) Sedimentological control on Mn, and other trace elements, in groundwater of the Bengal Delta. *Environ Sci Technol* 46:669–676
- Meybeck M (1987) Global chemical weathering of surficial rocks estimated from river dissolved loads. *Am J Sci* 287:401–428
- Mondal D, Gupta S, Reddy DV, Nagabhushanam P (2014) Geochemical controls on fluoride concentrations in groundwater from alluvial aquifers of the Birbhum district, West Bengal, India. *J Geochem Explor* 145:190–206

- Mukherjee B, Rao MG, Karunakaran C (1969) Genesis of kaoline deposits of Birbhum, West Bengal, India. *Clay Miner* 8:161–170
- Parkhurst DL, Appelo CAJ (1999) User's guide to PHREEQC (version 2)—a computer program for speciation, batch-reaction, one-dimensional transport, and inverse geochemical calculations. US Geological Survey Water-Resources Investigations Report 99-4259
- Patra PK, Mandal B, Chakraborty S (2010) Hydrogeochemistry of fluoride rich groundwater in Birbhum district of West Bengal, India. *Ecoscan* 4(2 and 3):209–211
- Pickering WF (1985) The mobility of soluble fluoride in soils. *Environ Pollut* 9:281–308
- Piper AM (1944) A graphic procedure in the geochemical interpretation of water analyses. *Am Geophys Union Trans* 25:914–923
- Rajmohan N, Elango L (2004) Identification and evolution of hydrogeochemical processes in the groundwater environment in an area of the Palar and Cheyyar River Basins, Southern India. *Environ Geol* 46:47–61
- Ramanaiah SV, Venkatamohan S, Rajkumar B, Sarma PN (2006) Monitoring of fluoride concentration in groundwater of Prakasham district in India: correlation with physicochemical parameters. *J Environ Sci Eng* 48:129–134
- Sawyer CN, McCarty PL (1967) *Chemistry of sanitary engineers*. McGraw Hill, New York
- Schoeller H (1965) Qualitative evaluation of groundwater resources. In: *Methods and techniques of groundwater investigations and development*. UNESCO, pp 54–83
- Schoeller H (1967) Geochemistry of groundwater. In: *An international guide for research and practice*. UNESCO, pp 1–18
- Sikdar PK, Chakraborty S (2008) Genesis of arsenic in groundwater of North Bengal Plain using PCA: a case study of English Bazar Block, Malda District, West Bengal, India. *Hydrol Process* 22:1796–1809
- Singh CK, Mukherjee S (2015) Aqueous geochemistry of fluoride enriched groundwater in arid part of Western India. *Environ Sci Pollut Res* 22:2668–2678
- Singh CK, Rina K, Singh RP, Shashtri S, Kamal V, Mukherjee S (2011) Geochemical modeling of high fluoride concentration in groundwater of Pokhran Area of Rajasthan, India. *Bull Environ Contam Toxicol* 86:152–158
- Srinivasa Rao N (1997) The occurrence and behaviour of fluoride in the groundwater of the Lower Vamsadhara River basin, India. *Hydrol Sci* 42(6):877–892
- Srinivasamoorthy K, Chidambaram S, Prasanna MV, Vasanthavihar M, Peter J, Anandhan P (2008) Identification of major sources controlling groundwater chemistry from a hard rock terrain—a case study from Mettur taluk, Salem district, Tamil Nadu, India. *J Earth Syst Sci* 117:49–58
- Stallard RF, Edmond JM (1983) Geochemistry of Amazon, the influence of geology and weathering environment on the dissolved load. *J Geophys Res* 88:9671–9688
- Subba Rao N (2009) Fluoride in groundwater, Varaha River Basin, Visakhapatnam District, Andhra Pradesh, India. *Environ Monit Assess* 152:47–60
- Subba Rao N (2011) High-fluoride groundwater. *Environ Monit Assess* 176:637–645
- Subba Rao N, Devadas DJ (2003) Fluoride incidence in groundwater in an area of Peninsula India. *Environ Geol* 45:243–251
- UNICEF (1999) States of the art report on the extent of fluoride in drinking water and the resulting endemicity in India. Report by Fluorosis and Rural Development Foundation for UNICEF, New Delhi
- Vengosh A, Keren R (1996) Chemical modifications of groundwater contaminated by recharge of sewage effluent. *J Contam Hydrol* 23:347–360
- Viero AP, Roisenberg C, Roisenberg A, Vigo A (2009) The origin of fluoride in the granitic aquifer of Porto Alegre, Southern Brazil. *Environ Geol* 56:1707–1719
- Wei C, Guo H, Zhang D, Wu Y (2015) Occurrence and hydrogeochemical characteristics of high-fluoride groundwater in Xiji County, southern part of Ningxia Province, China. *Environ Geochem Health*. doi:10.1007/s10653-015-9716-x
- Wen X, Wu Y, Zhang Y, Liu F (2005) Hydrochemical characteristics and salinity of groundwater in the Ejina Basin, Northwestern China. *Environ Geol* 48:665–675
- Wenzel WW, Blum WEH (1992) Fluoride speciation and mobility in fluoride contaminated soil and minerals. *Soil Sci* 153:357–364
- WHO (2011) *Guidelines for drinking-water quality*, 4th edn. World Health Organization, Geneva
- Yidana SM, Ophori D, Yakubo BB, Samed AA (2012) A factor model to explain the hydrochemistry and causes of fluoride enrichment in groundwater from the middle Voltaian sedimentary aquifers in the northern region, Ghana. *ARPN J Eng Appl Sci* 7(1):50–68